

Copy No. 0

NASA Program Apollo Working Paper No. 1109

ANALOG SIMULATION OF THE PILOT CONTROLLED  
RENDEZVOUS MANEUVERS FOR LEM

N70-76257  
ACCESSION NUMBER  
44  
PAGES  
TMX-6511  
NASA CR OR TMX OR AD NUMBER  
(THRU) none  
(CODE)  
(CATEGORY)

FACILITY FORM 602



NATIONAL AERONAUTICS AND SPACE ADMINISTRATION  
MANNED SPACECRAFT CENTER

Houston, Texas

March 12, 1964

NASA PROGRAM APOLLO WORKING PAPER NO. 1109

ANALOG SIMULATION OF THE PILOT CONTROLLED  
RENDEZVOUS MANEUVERS FOR LEM

Prepared By:

Ronald W. Simpson  
Ronald W. Simpson  
AST, Flight Dynamics Branch

George C. Guthrie  
George C. Guthrie  
AST, Control and Guidance Systems Branch

AUTHORIZED FOR DISTRIBUTION:

Harren Gillespie, Jr.  
for Maxime A. Faget  
Assistant Director for Engineering and Development

NATIONAL AERONAUTICS AND SPACE ADMINISTRATION

MANNED SPACECRAFT CENTER

HOUSTON, TEXAS

March 12, 1964

## TABLE OF CONTENTS

Section	Page
SUMMARY . . . . .	1
INTRODUCTION . . . . .	1
SYMBOLS . . . . .	2
DESCRIPTION OF SIMULATION . . . . .	4
General . . . . .	4
Guidance Equations . . . . .	5
Cockpit Displays . . . . .	5
Translational and Attitude Controllers . . . . .	6
Translational and Attitude Control Systems . . . . .	6
Characteristics of Simulated LEM . . . . .	7
TEST PROGRAM . . . . .	7
Test Conditions . . . . .	7
Run Schedule . . . . .	8
Rendezvous Procedure . . . . .	8
DISCUSSION OF TEST RESULTS . . . . .	9
General . . . . .	9
Effect of Guidance Law . . . . .	9
Hohmann Transfer Rendezvous . . . . .	10
Equipperiod Transfer Rendezvous . . . . .	10
Effect of Attitude Control System . . . . .	11
Recommended Thrusting Schedule . . . . .	11
CONCLUSIONS . . . . .	12
REFERENCES . . . . .	13
TABLE 1.- INITIAL CONDITIONS . . . . .	14
TABLE 2.- AVERAGE END CONDITIONS . . . . .	15
FIGURES 1 THROUGH 16 . . . . .	16
APPENDIX . . . . .	35

## LIST OF FIGURES

Figure		Page
1	Simulated LEM cockpit . . . . .	16
2	Rotating reference coordinate system centered in CSM . . . . .	17
3	Simulator flow diagram . . . . .	18
4	Instrument panel . . . . .	19
5	Attitude and translation controls . . . . .	20
6	LEM body axis system . . . . .	21
7	RCS jet configuration for LEM . . . . .	22
8	Pitch attitude control circuit (Att. hold, rate command, and open loop) . . . . .	23
9	Initial conditions for rendezvous from Hohmann type transfer cases . . . . .	24
10	Initial conditions for rendezvous from equiperiod type transfer cases . . . . .	25
11	Runs involving initial deviations from the Hohmann Transfer Ellipse with and without guidance (case H3) . . . . .	26
12	Runs involving initial deviations from the equiperiod transfer ellipse with and without guidance (case E2) . . . . .	27
13	Hohmann transfer rendezvous (case H1) (a) Typical trajectory flown with guidance (using ascent engine) . . . . . (b) Velocity profiles . . . . .	28 29
14	Hohmann transfer rendezvous (case H1) (a) Typical trajectory flown with guidance (using RCS jets) . . . . . (b) Velocity profiles . . . . .	30 31

## LIST OF FIGURES

Figure		Page
15	Equiperiod transfer rendezvous	
	(a) Typical trajectory flown with guidance . . . . .	32
	(b) Velocity profiles . . . . .	33
16	Recommended thrusting schedule for equiperiod rendezvous . . . . .	34

## ANALOG SIMULATION OF THE PILOT CONTROLLED RENDEZVOUS MANEUVERS FOR LEM

### SUMMARY

The rendezvous of a pilot controlled LEM spacecraft with a lunar orbiting CSM spacecraft was simulated in six-degrees-of-freedom using an analog computer and a fixed-base simulator containing the pilot controls and instrument displays. Guidance velocity information computed from linearized gravity equations was used to aid the pilot in rendezvousing with the CSM from both Hohmann and equiperiod type transfers.

Results of the study indicate that the guidance equations did aid the pilot in executing the maneuver from both types of transfer orbits; however, the study also reveals that the  $\Delta V$  used to complete the rendezvous using the guidance was almost twice the theoretical minimum  $\Delta V$  necessary to perform the same maneuver. This was in part caused from having to thrust along individual axes. Injection thrusting from a Hohmann transfer ellipse was made equally well with either the ascent engine or RCS jets, but the  $\Delta V$  expenditure increased slightly using RCS jets. The best technique found for injecting from an equiperiod transfer ellipse was to thrust with the ascent engine first to lower closing velocities and then use the RCS jets to complete the rendezvous.

For a minimum  $\Delta V$  change, injection thrusting, as the study showed, should be delayed until the instant before intercept occurs, but to assure pilot safety it must be initiated at a finite range. In rendezvousing from the Hohmann transfer, the injection thrusting should be started at a range of about 5 nautical miles using the RCS jets since the relative velocities are low. However, for the equiperiod transfer, injection thrusting should be initiated at a range of about 13 nautical miles so that the RCS jets can be used to complete the maneuver if the ascent engine fails.

### INTRODUCTION

Successful lunar landing Apollo missions as now proposed require a rendezvous of the Lunar Excursion Module (LEM) with the Command Service Module (CSM) in circular orbit about the moon. To effect this rendezvous maneuver, a guidance system must be available to control the LEM during the time the maneuver is being executed.

Previous studies have investigated several types of guidance and displays that could be used to perform the rendezvous maneuver (refs. 1 and 2). Reference 1 evaluated the ability of a pilot to achieve a rendezvous through pilot displays of elevation and azimuth angles, their angular rates, range and range rate. Another study (ref. 2) used only range and range rate pilot information. Both these studies assumed that thrusting was confined to the longitudinal axis of the commuter spacecraft.

It is also possible, however, to compute guidance velocity information as a function of time to intercept and the present position of the LEM and to display these velocity components to the pilot for guidance purposes. By matching the actual velocity components with the displayed guidance quantities, the pilot is able to place the LEM on a coasting intercept trajectory. Within the last mile before intercept would occur the guidance information is disabled and the pilot performs the remainder of the maneuver by monitoring range and range rate directly.

To provide information on the usefulness of this type of guidance information for rendezvous, a simulation of the lunar orbit rendezvous maneuver was conducted by the Control and Guidance Systems Branch and the Flight Dynamics Branch, Guidance and Control Division. It is the purpose of this document to present the results of this simulation.

#### SYMBOLS

A	Rotational matrix which transforms vector quantities from the body axis system to the reference axis system.
C	Effective exhaust velocity, gIsp, ft/sec
g	Acceleration of gravity at earth sea level, ft/sec <sup>2</sup>
I <sub>sp</sub>	Specific impulse, sec
I <sub>x<sub>b</sub></sub> , I <sub>y<sub>b</sub></sub> , I <sub>z<sub>b</sub></sub>	LEM moments of inertia with respect to the X <sub>b</sub> , Y <sub>b</sub> , and Z <sub>b</sub> axes, slug-ft <sup>2</sup>
l <sub>φ</sub> , l <sub>θ</sub> , l <sub>ψ</sub>	Roll, pitch and yaw moments arms, ft
m	Mass of LEM, slugs
M <sub>p</sub>	Mass of propellant used in making ΔV change, slugs

$M\phi, M\theta, M\psi$	Roll, pitch and yaw control moments about the LEM body axis, ft-lb
$p, q, r$	Roll, pitch and yaw rates of LEM about the $(X_b, Y_b, Z_b)$ axis, deg/sec
$p_t, q_t, r_t$	Components of the total turning rate of LEM with respect to inertial space referred to the LEM body axis system, deg/sec. (See equations A21, A22, and A23 in Appendix)
$r_f$	Position vector of LEM with respect to center of moon
$r_s$	Position vector of CSM with respect to center of moon
$R$	Range along line of sight from LEM to the CSM, ft
$t$	Elapsed time, sec
$T$	Thrust, lb
$T_{x_b}, T_{y_b}, T_{z_b}$	Translational thrust of LEM engines along $X_b, Y_b$ , and $Z_b$ axes respectively, lb
$T_{x_I}, T_{y_I}, T_{z_I}$	Translational thrust of LEM engines referred to the reference axis system, lb
$T\psi, T\theta, T\phi$	Thrust producing angular acceleration about $X_b, Y_b$ , and $Z_b$ axes, lb
$\Delta V$	Change in relative velocity of LEM with respect to CSM, ft/sec
$(X_b, Y_b, Z_b)$	LEM body axis system
$(X_I, Y_I, Z_I)$	Displacements measured in reference axis system located in command module, ft. (The $Z_I$ axis is perpendicular to the plane of the orbit. The $X_I$ and $Y_I$ axes lie in the plane of the orbit with $Y_I$ always pointing away from the center of the moon and the $X_I$ axis pointing opposite to the direction of the orbital velocity of the command module.)



$\dot{X}_{GI}, \dot{Y}_{GI}$	Calculated reference velocities used for guidance purposes in the rendezvous maneuver, ft/sec
$\lambda$	Spacecraft mass ratio, $\frac{m_o}{m_o - M_p}$
$\sigma$	Standard deviation
$\tau$	Time to intercept, sec
$\phi, \theta, \psi$	Angular displacements of LEM about the $(X_b, Y_b, Z_b)$ axis system, degrees
$\omega_s$	Turning rate of the reference axis system necessary to keep the $Y_I$ axis directed away from the center of the moon, rad/sec

#### Subscripts

a	Actual
b	Relative to LEM body axis system
I	Relative to reference axis system
o	Initial condition

A bar over a quantity denotes a vector.

A dot over a quantity denotes first derivative with respect to time; two dots denote a second derivative with respect to time.

### DESCRIPTION OF SIMULATION

General.- The rendezvous simulation was implemented by coupling an analog computer solution of the six-degrees-of-freedom equations of motion of the LEM relative to the CSM with a simulated LEM cockpit. The cockpit as shown in fig. 1, was equipped with attitude and translational controllers and instrument displays of the parameters which described the relative motion of the LEM. The equations of motion (see Appendix) are derived for a rotating set of reference axes, as shown in fig. 2, whose origin is located at the CSM center of mass. The derivation of these equations, for which a linear gravity was assumed, can be found in ref. 3. For the purposes of this simulation, the CSM was assumed to be in an 80 nautical mile circular orbit. The pilot's task was to

control the LEM using the guidance velocity information to achieve a given set of end conditions. The pilot accomplished this by thrusting with the RCS and/or ascent engine to match the actual spacecraft velocities with the guidance velocities. A flow diagram of the complete simulation is shown in fig. 3.

Guidance Equations. - The guidance equations used in this simulation were derived, as shown in the Appendix, from the linearized equations of motion by setting the thrusting terms equal to zero. These equations were solved for guidance velocities as a function of present position and time to a nominal intercept point. The following reference expressions were obtained:

$$\dot{X}_{GI} = \omega_s \left[ \frac{X_I \sin \omega_s \tau + Y_I [\omega_s \tau \sin \omega_s \tau - 14 (1 - \cos \omega_s \tau)]}{3 \omega_s \tau \sin \omega_s \tau - 8(1 - \cos \omega_s \tau)} \right] \quad (1)$$

$$\dot{Y}_{GI} = \omega_s \left[ \frac{2X_I (1 - \cos \omega_s \tau) + Y_I (4 \sin \omega_s \tau - 3\omega_s \tau \cos \omega_s \tau)}{3 \omega_s \tau \sin \omega_s \tau - 8(1 - \cos \omega_s \tau)} \right] \quad (2)$$

Cockpit Displays. - The pilot information display panel used in this simulation is shown in fig. 4. The instruments used consisted of a 3-axis attitude and rate indicator, 3 position meters, 3 reference velocity meters, 3 measured velocity meters, a stop clock, a main engine fuel meter, and an RCS fuel meter.

Functions of the instruments are as follows:

1. Attitude and rate indicator - Provided roll, pitch and yaw attitude of the LEM with respect to the CSM. The rotational sequence from the reference axis system to the LEM body axis system was pitch, yaw and roll. LEM body rates ( $p_t$ ,  $q_t$ ,  $r_t$ ) were displayed on the rate indicators.

2. Position meters - Indicated the position of the LEM relative to the CSM along the reference  $x_I$ ,  $y_I$ ,  $z_I$  axes.

3. Guidance velocity meters - Displayed the guidance relative velocities ( $\dot{X}_{GI}$ ,  $\dot{Y}_{GI}$ ) of the LEM along the reference trajectory. These meters presented solutions of the guidance equations.

4. Measured velocity meters - Displayed measured relative velocities ( $\dot{X}_I$ ,  $\dot{Y}_I$ ,  $\dot{Z}_I$ ) of the LEM in the reference coordinate system.

5. Stop-clock - Allowed the pilot to monitor elapsed time of the run.

6. Fuel meters - Provided the pilot with information regarding the percentage of translational and attitude fuel remaining at any instant in both the ascent engine tanks and RCS tanks.

Translational and Attitude Controllers. - The vehicle controls shown in fig. 5, consisted of a three-axis translational controller and a three-axis attitude controller. The translational RCS jets, which gave translational acceleration along the body axes, were controlled by the pilot directly through the left hand controller. This same controller also operated the 5,000 lb thrust ascent engine by repositioning a toggle switch on the instrument panel. The ascent engine could be operated by pulling vertically upward (with respect to the pilot) on the translational controller. Translational acceleration from the ascent engine was directed along the positive LEM X-body axis (see fig. 6).

The attitude controller operated by the pilot's right hand also fired the RCS jets to provide angular acceleration about the LEM body axes. A deadband of  $\pm 5$  percent full stick deflection was used in this controller to prevent inadvertent operation of the RCS jets.

Translational and Attitude Control Systems. - The pilot controlled the translational RCS jets open loop. Operation of these jets was by on-off thrusting. The RCS jet configuration used in this simulation is shown in fig. 7.

Operation of the attitude control jets was also by on-off thrusting. Three modes of control were possible with the attitude control system: (1) rate command with attitude-hold, (2) rate command, and (3) open-loop. The switching circuits used for the activation of the on-off thrusters incorporated a deadband of  $\pm 2$  degrees in attitude hold and .5 degrees per second in the rate command system. The maximum angular acceleration rates in open-loop were  $54 \text{ degrees/sec}^2$ ,  $29.22 \text{ degrees/sec}^2$ , and  $25.78 \text{ degrees/sec}^2$  about the  $X_b$ ,  $Y_b$ , and  $Z_b$  axes, respectively. A maximum rate of 20 degrees/sec was assumed for the rate-command mode. In attitude-hold mode, the attitude feedback signal was made proportional to the direction cosines obtained from the matrix transformation. This allowed the attitude hold circuits to function properly over a wide range of angular variations. Figure 8 illustrates the pitch axis mechanization of the attitude control system; the roll and yaw axes mechanizations were similar except for inputs. The logic box shown in fig. 8 directed the rotational and translational control signals to the proper RCS jet to prevent simultaneous ignition of opposing jets.

Characteristics of Simulated LEM. - The LEM simulated for the purpose of this study had the following physical characteristics:

Mass = 141.8 slugs (including 19.4 slugs of fuel)

$$I_{zb} = 2,260 \text{ slug-ft}^2$$

$$I_{yb} = 1,990 \text{ slug-ft}^2$$

$$I_{xb} = 1,174 \text{ slug-ft}^2$$

No center-of-gravity offset or changes were assumed. The RCS jets gave a thrust of 100 pounds each with a total thrust of 200 pounds maximum along any one axis. A thrust of 5,000 pounds could be obtained along the positive  $X_b$  axis using the ascent engine. The RCS jets and the ascent engine produced translational accelerations of  $1.42 \text{ ft/sec}^2$  and  $35.46 \text{ ft/sec}^2$  respectively. A multistart capability was assumed for the ascent engine.

As currently proposed, the LEM ascent engine will have a thrust of 3,500 pounds. At the time this study was initiated, however, the LEM ascent engine was proposed to have a thrust of 5,000 pounds. Since digital computer runs were made with a 5,000 pound thrust engine and the results from these runs were used for comparison with the analog simulation results, the ascent engine thrust level used in the analog simulation also had to be set at 5,000 pounds. The specific impulse used was 305 seconds.

It was assumed that radar and computer equipment were onboard LEM and functioning perfectly to obtain the information displayed to the pilot. This information was not degraded in any manner, such as with noise.

## TEST PROGRAM

Test Conditions. - Simulated rendezvous maneuvers were made from Hohmann and equipperiod type transfer orbits. Initial conditions which represented large perturbations from these nominal transfer orbits were also used in some runs. Table 1 contains a summary of the initial conditions used. Case H1 placed the LEM on the nominal or ideal Hohmann transfer orbit and cases H2 through H4 represented perturbed conditions

off the Hohmann transfer. Out-of-plane ( $Z_I$ ) errors were used in cases H3 and H4. The initial relationship of LEM and CSM for the Hohmann and near Hohmann transfer cases is shown pictorially in fig. 9. Case E1 had initial conditions which corresponded to the ideal equiperiod transfer orbit for the LEM and cases E2 and E3 represented perturbed conditions off the equiperiod transfer orbit. No out-of-plane errors were used in these three runs. A diagram of the relative initial positions of LEM and CSM for the equiperiod and near equiperiod cases is shown in fig. 10. The large initial velocity errors used in this simulation are unrealistic considering the relatively small range errors which were also used; however, they served the purpose of burdening the guidance task to determine the effect on pilot performance. The initial time to intercept for all runs was held constant at 600 seconds. In order to satisfy this restriction the Hohmann and equiperiod type runs were started at maximum ranges of 65,000 feet and 250,000 feet respectively.

In the Hohmann transfer case, the rendezvous maneuver was considered complete when the range was less than 100 feet and the velocity was less than 1 ft/sec. The equiperiod transfer runs were assumed completed when the range was below 1,000 feet with the relative velocity less than 10 ft/sec. The difference in these two types of end conditions was the result of analog computer scaling limitations.

Run Schedule.- Altogether, two pilots made a total of 93 runs. Fifty-nine of these runs were made from the Hohmann and off Hohmann transfer orbits, four of which were without guidance. Of the thirty-four runs made from the equiperiod type transfer orbits, five were without guidance. A major portion of all the runs utilized either an attitude hold or a rate command attitude control system; however, eleven of the runs were made with an open loop attitude control system.

Rendezvous Procedure.- For the runs in which the guidance displays were operative, both pilots used approximately the same type of rendezvous procedure. This procedure consisted of initially matching the actual LEM relative velocities and guidance relative velocities by commanding thrust as required. Once these velocities were matched, the pilot allowed the LEM to coast along the trajectory until a range was reached where thrusting was required to inject the LEM into the CSM orbit. This range depended on what combination of RCS jets and ascent engine was used for the thrusting.

The runs which were made without guidance displays in operation were done so to determine how effective the guidance displays were in assisting the pilot in executing a rendezvous. In these runs, the pilot performed the rendezvous by monitoring only the actual LEM relative velocity and displacement meters. The pilot attempted to control the spacecraft so that the  $X_I$ ,  $Y_I$ , and  $Z_I$  range and range rate components reached zero simultaneously.

## DISCUSSION OF TEST RESULTS

General. - In analyzing the data obtained from this simulation, pilot performance was evaluated primarily by the total  $\Delta V$  made during the rendezvous maneuver as compared to the theoretical minimum  $\Delta V$  necessary to execute the maneuver. The theoretical minimum  $\Delta V$  values were obtained from digital computer runs using a bilinear acceleration program for the terminal rendezvous. From these runs the theoretical minimum  $\Delta V$  for the Hohmann and equiperiod transfer rendezvous were found to be 98.5 ft/sec and 372 ft/sec respectively. In order to convert fuel usage, obtained from the analog simulation, to an equivalent  $\Delta V$ , the following equation was used:

$$\Delta V = C \ln \lambda \quad (3)$$

This study indicated that displaying reference velocity information aided the pilot in accomplishing the rendezvous maneuver. The study also revealed, however, that the pilot used approximately twice the  $\Delta V$  theoretically required to execute the maneuver. In the case of the ideal Hohmann transfer rendezvous, an average  $\Delta V$  of the 189 ft/sec was used while the minimum  $\Delta V$  required is 98.5 ft/sec. The average  $\Delta V$  used in the ideal equiperiod transfer rendezvous was 618 ft/sec, whereas, theoretically, the rendezvous can be made with a  $\Delta V$  of 372 ft/sec. The average end conditions for all cases investigated are given in table 2.

By allowing the pilots to vary the thrusting schedule for the terminal rendezvous, it was determined that the Hohmann transfer rendezvous could be made using either the ascent engine or the RCS jets because of the low  $\Delta V$  required. In the equiperiod rendezvous case, however, it was necessary to use the ascent engine to lower the range rate to a level which could be handled more easily by the RCS jets. The maneuver can also be made using the RCS jets alone, but at an increased  $\Delta V$  expenditure.

All runs made from both the Hohmann and equiperiod type transfers yielded high  $\Delta V$  changes when compared with the theoretical minimum  $V$ . Some of this  $\Delta V$  can be attributed to the fact that the guidance velocity was displayed in components, consequently the velocity changes had to be made by components. A large portion of the excessive  $\Delta V$ , however, was due to pilot inefficiency. Some runs were flown with a  $\Delta V$  change well below the averages and some were well above the averages. This is verified by the standard deviation values given for the  $\Delta V$  averages in table 2. These results indicate that pilot errors were costly.

Effect of Guidance Law. - As stated earlier most of the simulation runs were made with guidance; however, a few were made without guidance

to indicate the effectiveness of the guidance equations. Typical results for two cases (H3 and E2) ran with and without guidance are illustrated in figs. 11 and 12. Large initial velocity errors were used in these cases, not because this can occur in the real situation, but rather to burden the guidance task for the maneuver. In both cases a significant reduction in  $\Delta V$  change (341 and 198 fps for the cases shown) is obtained by using the guidance equations. In performing rendezvous without guidance information, pilot performance was primarily dependent upon how well the initial velocity correction was accomplished.

Hohmann Transfer Rendezvous. - A typical rendezvous trajectory from the ideal Hohmann transfer ellipse (case H1) using guidance is shown in fig. 13a. Thrusting for the run was accomplished with the ascent engine and the point at which thrust was applied can be seen in fig. 13b. In a Hohmann transfer,  $Y_I$  and  $\dot{Y}_I$  go to zero simultaneously, but  $X_I$  increases as  $X_I$  nears intercept. Therefore, in this type of rendezvous, the thrust must be directed along the  $X_I$  axis. The  $\Delta V$  used in this run was 195 ft/sec.

Another rendezvous from the ideal Hohmann transfer using guidance and the RCS jets alone is shown in fig. 14a. As can be seen in fig. 14b, thrusting was initiated at a greater range in this run than it was when the ascent engine was used. The  $\Delta V$  required to make the rendezvous was 230 fps which is somewhat greater than the average. The larger  $\Delta V$  occurred because the LEM deviated from the ideal trajectory more than if the ascent engine had been used since thrusting was started at a greater range.

Equiperiod Transfer Rendezvous. - It was found to be very difficult to complete the rendezvous maneuver from the equiperiod transfer ellipse using only the RCS jets before all the available fuel was used. The reason for this is that the equiperiod transfer case involves much higher relative velocities than the Hohmann transfer case. The pilot found it much easier to make a large part of the  $\Delta V$  change with the ascent engine, thus his performance was more efficient.

A typical rendezvous trajectory flown with guidance from the ideal equiperiod transfer orbit is shown in fig. 15a. The  $\Delta V$  required to execute this rendezvous was 627 fps and the point at which thrust was applied is shown in fig. 15b. From this figure, it can be seen that in the equiperiod transfer  $\dot{X}_I$  and  $\dot{Y}_I$  go to zero simultaneously and thus thrusting must be directed along the  $Y_I$  axis.

In considering the rendezvous made from the equiperiod orbit, it must be noted that the LEM mass (141 slugs) was the same as that used in

the Hohmann runs. This is a lighter configuration than will exist in actual conditions for an equiperiod transfer rendezvous. Moreover, the ascent engine thrust level of 5,000 pounds was 1,500 pounds higher than the actual LEM ascent engine. Thus, the acceleration capabilities during a true equiperiod rendezvous will be lower than those used in this simulation. Even with this higher acceleration capability it was found that the ascent engine should be used to reduce most of the initial velocity difference to prevent large expenditures of  $\Delta V$ .

Effect of Attitude Control System.- Three types of attitude control systems - attitude-hold, rate-command, and open-loop - were used to evaluate their effect on the pilot's ability to execute the maneuver. Pilot performance was roughly the same using either the attitude-hold or rate-command systems, but the open-loop attitude control system complicated the pilot's task because of the relatively large control accelerations. The average weight of attitude fuel used in all the runs made was 6.08 pounds. The maximum used in any one run was 20.77 pounds and occurred during a rendezvous using open-loop attitude control.

Recommended Thrusting Schedule.- If a minimum  $\Delta V$  expenditure were the primary consideration in the rendezvous maneuver, the injection thrusting should be initiated at the last possible moment (seconds before impact with CSM) since there is less deviation from the ideal trajectory when thrusting is started closer to the intercept point. However, a major factor in considering any thrusting schedule is pilot safety. If thrusting were delayed to a range at which the rendezvous could be made only by using the ascent engine, and if the ascent engine were to fail, then the rendezvous would be very difficult to complete from such a short range using only the RCS jets. It should be kept in mind that the range to the intercept point was restricted in this problem because the time to intercept ( $\tau$ ) was held constant. If the optimum time to intercept had been computed by the method given in ref. 5, the range limit would not have existed and the  $\Delta V$  changes made probably would have been smaller. If the LEM were on a Hohmann transfer and this occurred, the rendezvous would still have to be made on that orbit because on the next orbit the LEM would be farther away from the CSM. In this case, the LEM would have to catch up to the CSM because the CSM would pass the LEM before the RCS jets could inject the LEM into the CSM orbit. If an equiperiod transfer were being flown and this failure occurred, it would probably be possible to make another orbit and start the thrusting at a greater range with the RCS jets during the next pass.

There is also the problem of not being able to see the CSM from the LEM, either visually or with radar, when the ascent engine is used because of the attitude which must be maintained during thrusting. This also makes it desirable to thrust with the ascent engine at a greater



range so that the LEM can be turned around before final thrusting with the RCS jets is required.

A thrusting schedule which could be used for the rendezvous maneuver from the equiperiod transfer is shown in fig. 16. This schedule is based on a LEM mass of 251.6 slugs and an ascent engine thrust of 3,500 pounds which are considered to be more representative of the true LEM for the equiperiod case than those values used in this simulation. Thrusting should be initiated with the ascent engine at approximately 13 nautical miles to inject the LEM into the CSM orbit. Ascent engine thrust is terminated at a closure rate of 150 fps. If the ascent engine fails, then 4 RCS jets can be used from the same range, except that thrusting is stopped at a range rate of 100 fps. After either of these periods of thrust a coasting period exists and there is still enough range (time) available to turn the LEM around to obtain visual and radar contact before thrusting is required again. The final thrusting with the RCS jets from a range of 5 nautical miles depends on individual pilot preference (the profile indicated in this region is for illustrative purposes).

In the Hohmann transfer case, it is expected that the range rate will be less than 150 fps at a range of 5 nautical miles and thus two RCS jets are sufficient for the thrusting task required since the LEM mass will be only about 141 slugs. Thus, the thrust schedule will be quite similar to the last phase (from 5 n. mi) of the thrust schedule for the equiperiod transfer and requires only two RCS jets. This allows visual and radar contact to be maintained during the entire terminal maneuver.

## CONCLUSIONS

1. The linearized set of guidance equations used in this simulation was effective in aiding the pilot to perform the rendezvous maneuver even when large initial-condition errors were assumed.
2. The total  $\Delta V$  expended to perform the rendezvous maneuver even with the guidance displays operating, average almost twice the theoretical minimum  $\Delta V$  required to make the maneuver. This  $\Delta V$  expenditure could probably be reduced if the guidance velocities were resolved into one resultant velocity and displayed as such.
3. Pilot performance was the same using either an attitude-hold or a rate-command attitude control system; however, the open-loop attitude control system complicated the pilots task somewhat because of the relatively large control accelerations available.

## REFERENCES

1. Brissenden, Roy F., Burton, Bert B., Foudriat, Edwin C., and Whitten, James B.: Analog Simulation of a Pilot-Controlled Rendezvous. NASA TN D-747, 1961.
2. Brissenden, Roy F., and Lineberry, Edgar C., Jr.: Visual Control of Rendezvous. (Written for presentation at the Thirtieth Annual Meeting of the IAS.) 1962.
3. Eggleston, John M. and Beck, Harold D.: A Study of the Positions and Velocities of a Space Station and a Ferry Vehicle During Rendezvous and Return. NASA TR R-87, 1961.
4. Clohessy, W. H. and Wiltshire, R. S.: Terminal Guidance System for Satellite Rendezvous. Jour. Aerospace Sci., September 1960, pp. 653-658.
5. Eggleston, John M.: Optimum Time to Rendezvous. Vol. 30, No. 11, ARS Journal, November 1960.
6. Eggleston, John M.: Extensions of Optimum Time to Rendezvous Studies. (For presentation at the Intercent Rendezvous Discussions, February 27-28, 1961.)
7. Hackler, Clarke T., Guthrie, George C., and Moore, Thomas E.: Preliminary Study of the Pilot-Controlled LEM Docking Maneuver. NASA Project Apollo Working Paper No. 1075, 1963.
8. Willman, J. L.: A Simulation Study of the Control Problems Encountered When Docking the LEM with the Command Module-Service Module Combination. Report No. NA63H-82, North American Aviation, Inc.

TABLE 1.- INITIAL CONDITIONS

Case	Trajectory	$\dot{X}_I$ ft/sec	$\dot{Y}_I$ ft/sec	$\dot{Z}_I$ ft/sec	$X_I$ feet	$Y_I$ feet	$Z_I$ feet
H1	Hohmann	+ 47.863	+ 96.615	0	- 48,883	- 29,636	0
H2	Hohmann	+308.545	+ 93.875	0	- 46,439	- 28,154	0
H3	Hohmann	-212.818	+ 99.355	-50	- 51,327	- 31,118	+3000
H4	Hohmann	-212.818	+ 30.000	+50	- 51,321	- 31,118	+3000
E1	Equiperiod	+371.147	-311.254	0	-118,396	+209,554	0
E2	Equiperiod	+116.412	-331.874	0	-124,316	+199,077	0
E3	Equiperiod	+625.882	-290.634	0	-112,477	+220,033	0

TABLE 2.- AVERAGE END CONDITIONS

Test Case	Translational Fuel			Attitude Fuel-lb	Elapsed Time-sec	Range Feet
	lb	$\Delta V$	lb			
H1	86.88	189 fps	24.53	5.01	759.22	48.72
H2	235.26	519 fps	40.48	5.05	711.43	51.99
H3	243.89	539 fps	30.14	9.14	788.91	31.73
H4	320.76	716 fps	32.17	7.88	752.27	64.66
E1	278.86	618 fps	52.71	4.92	807.53	476.34
E2	418.28	944 fps	38.66	5.99	855.31	503.34
E3	503.67	1148 fps	79.94	4.29	848.80	597.63

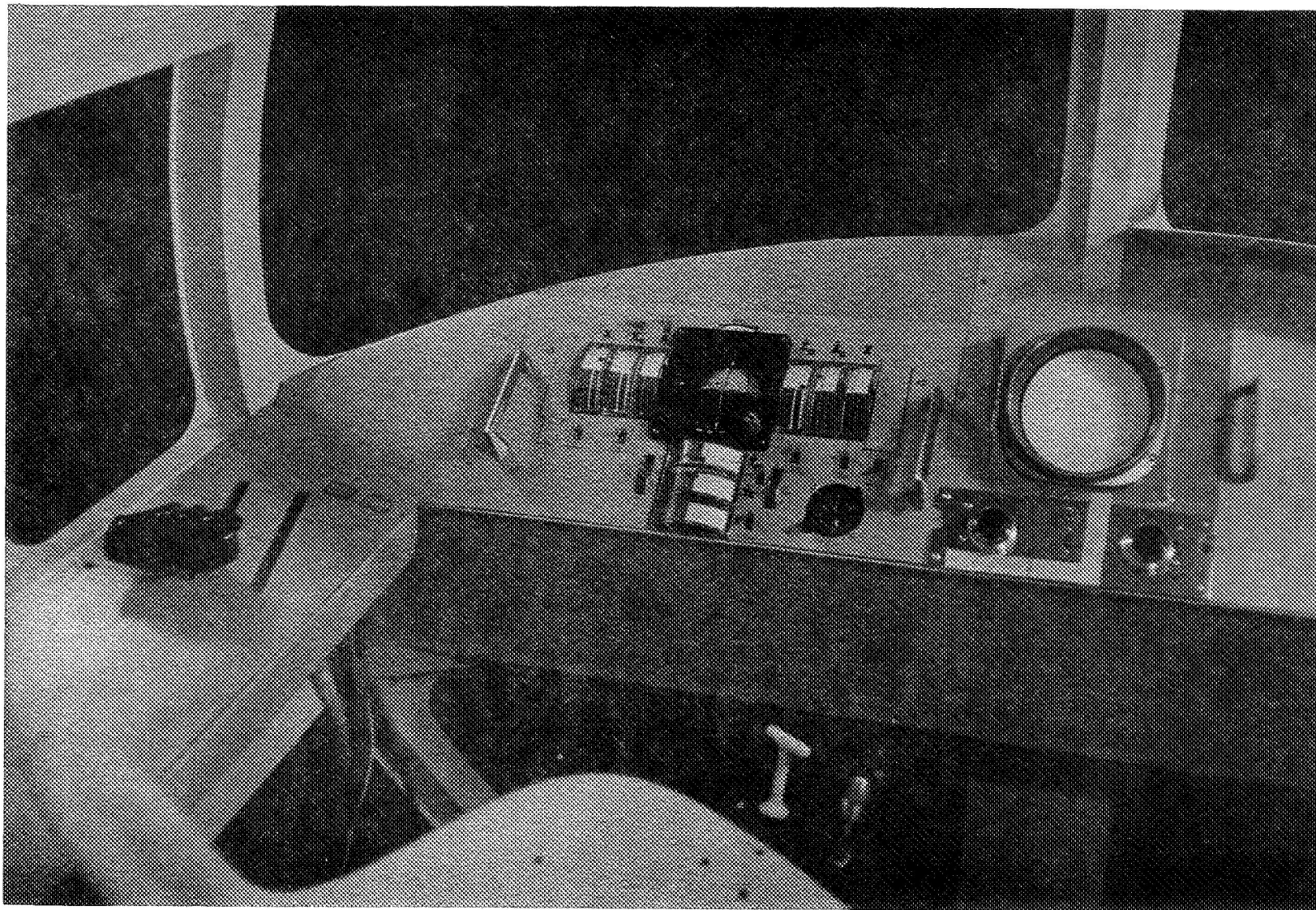


Figure 1.- Simulated LEM cockpit.

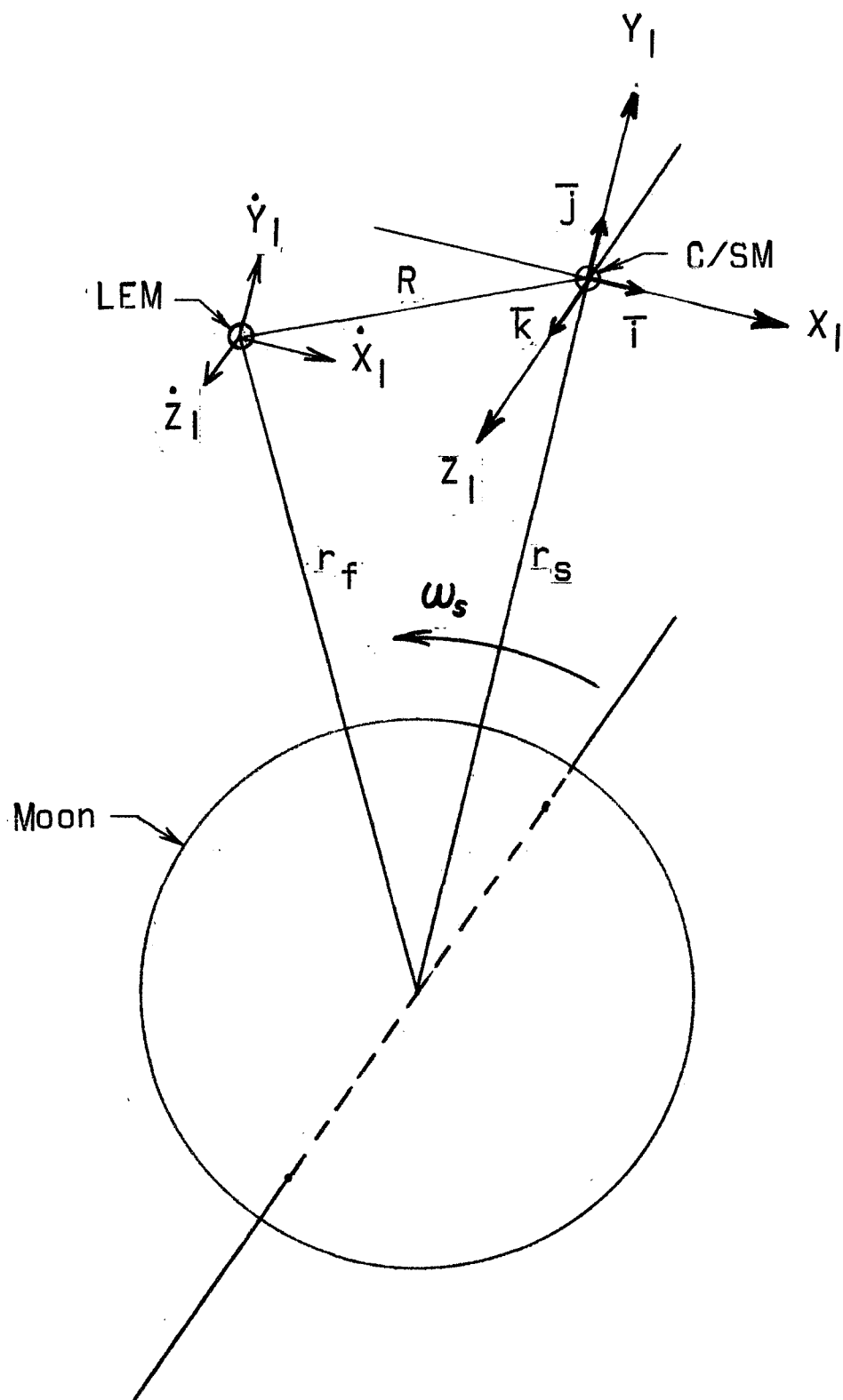


Figure 2.- Rotating reference coordinate system centered in CSM.

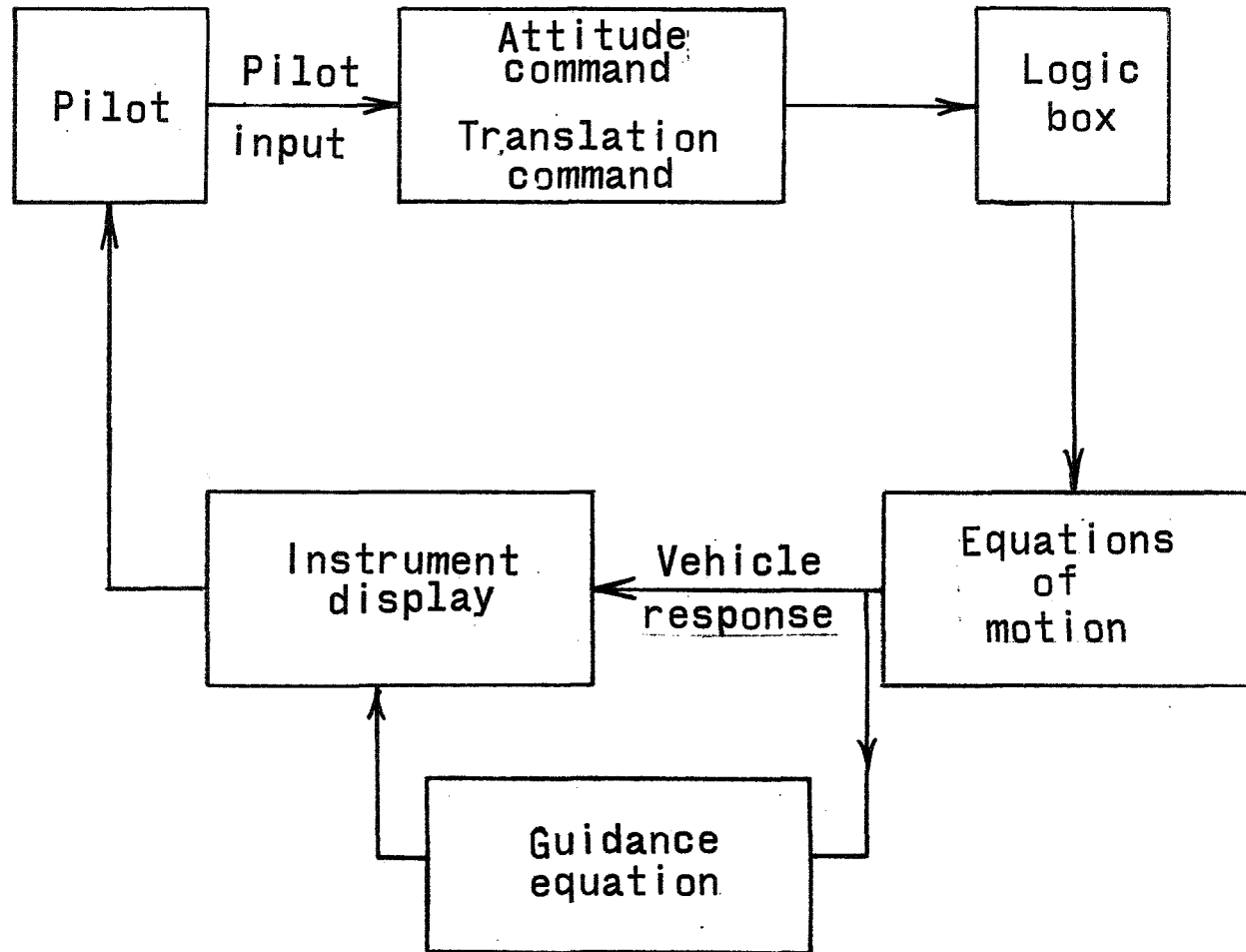


Figure 3.- Simulator flow diagram.

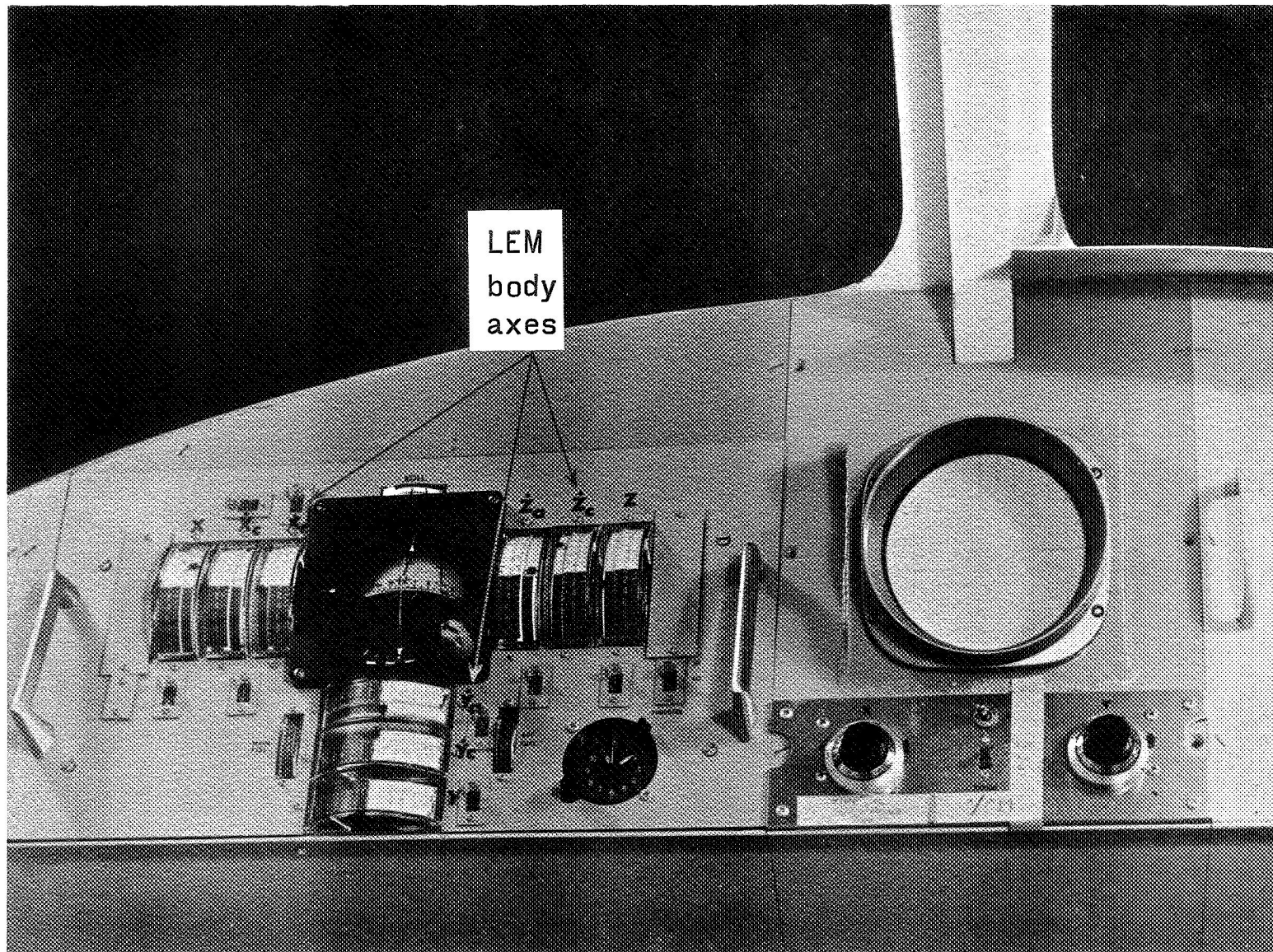


Figure 4.- Instrument panel.



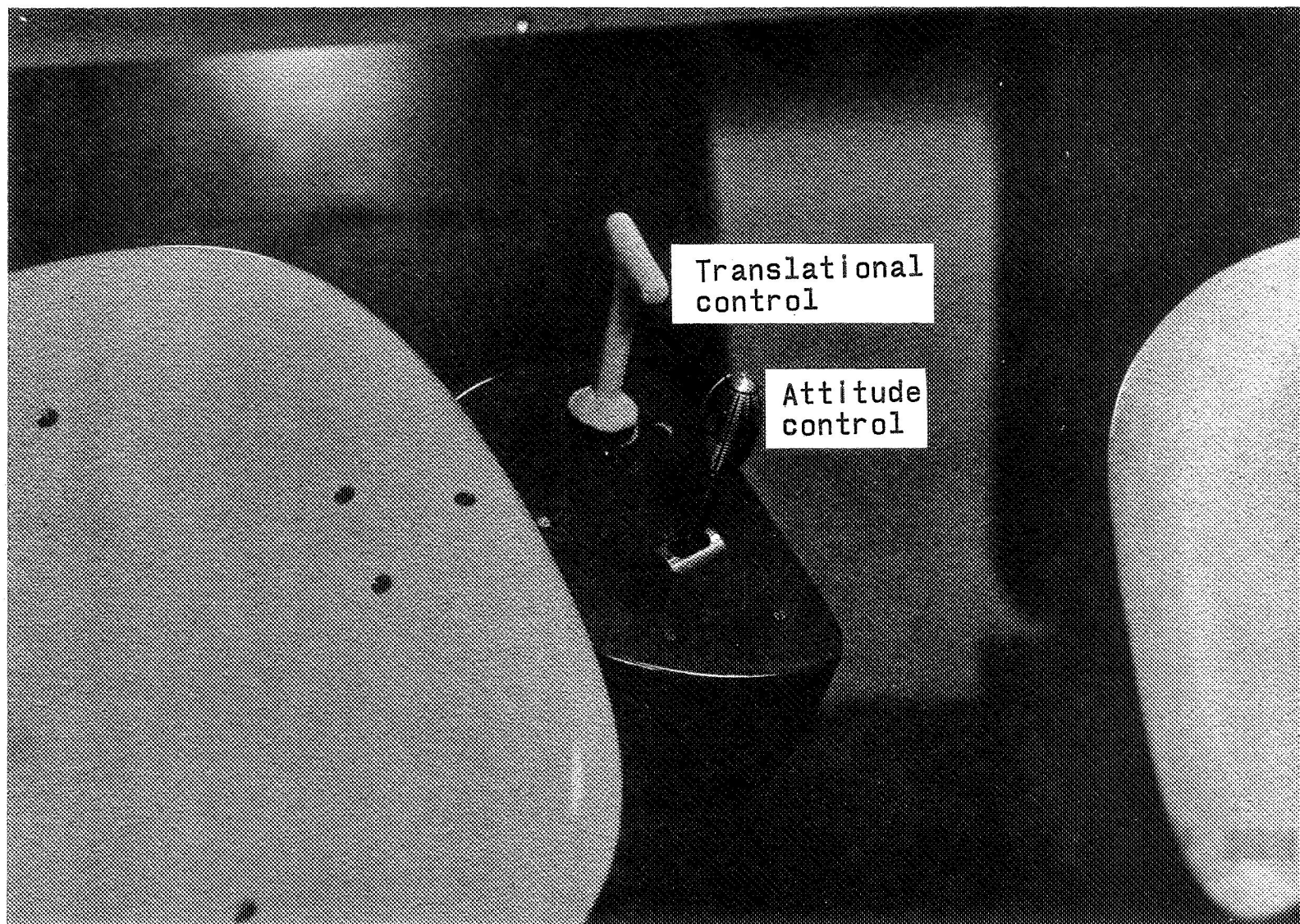


Figure 5.- Attitude and translation controls.

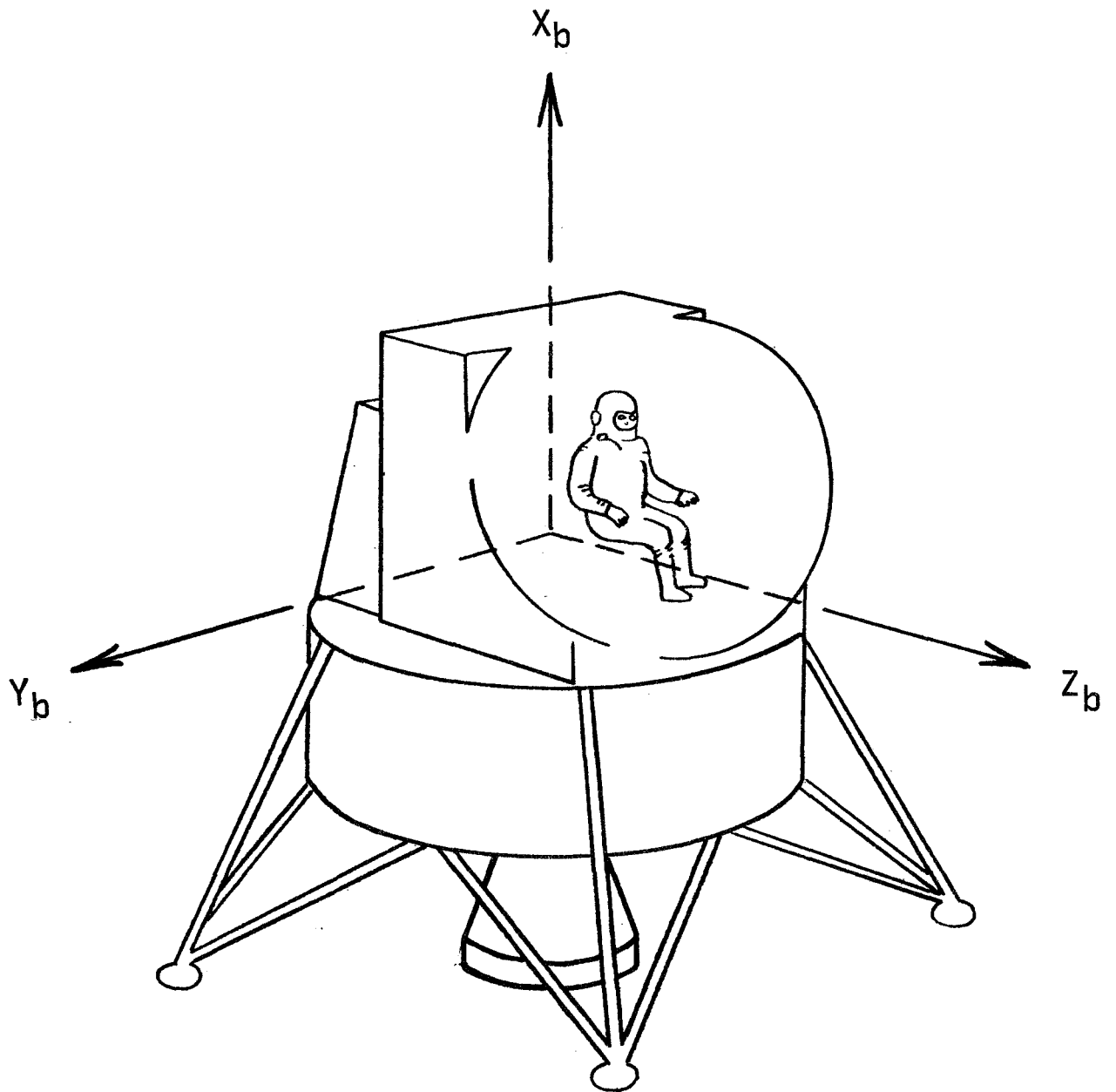


Figure 6.- LEM body axis system.

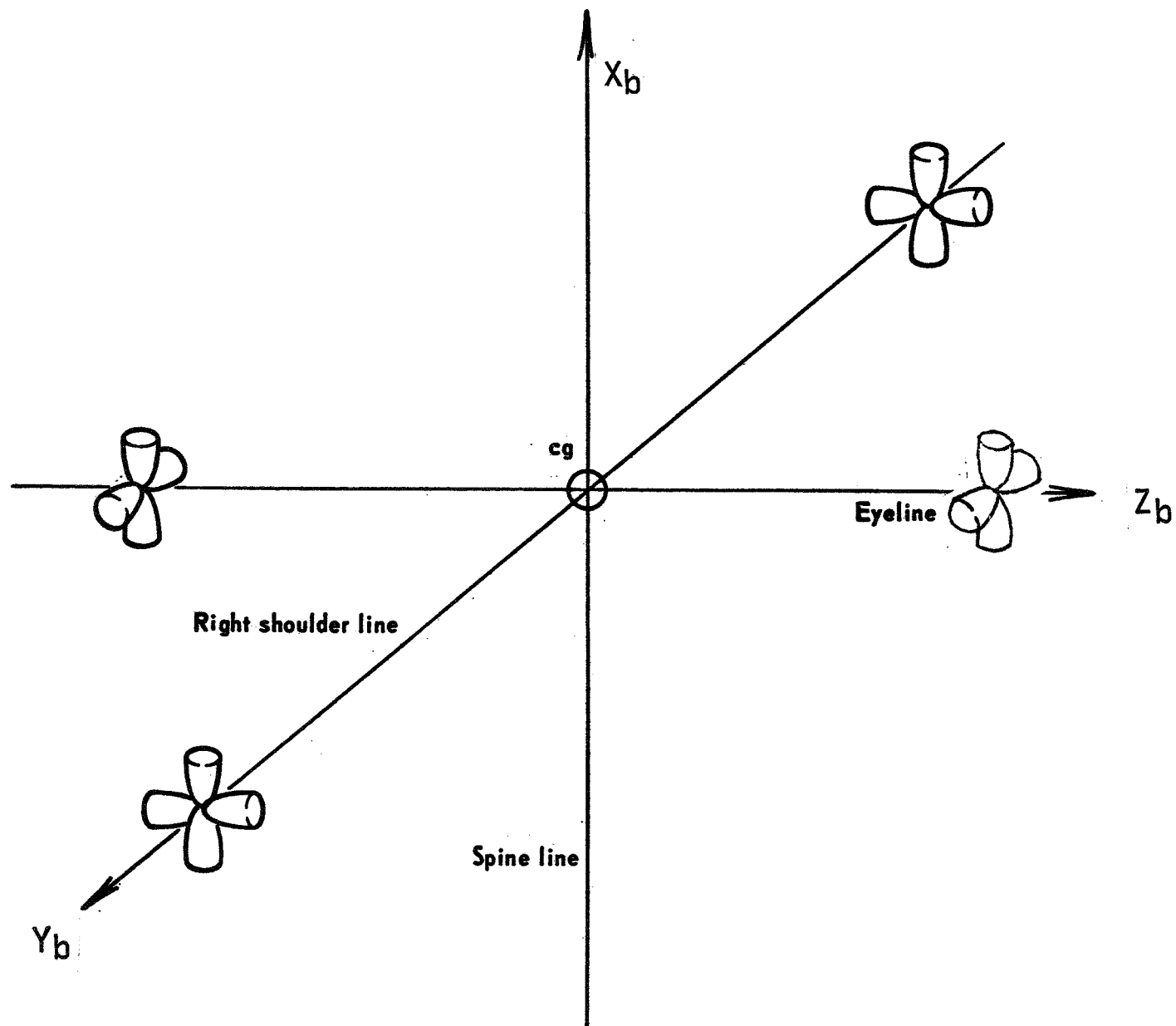


Figure 7.- RCS jet configuration for LEM.

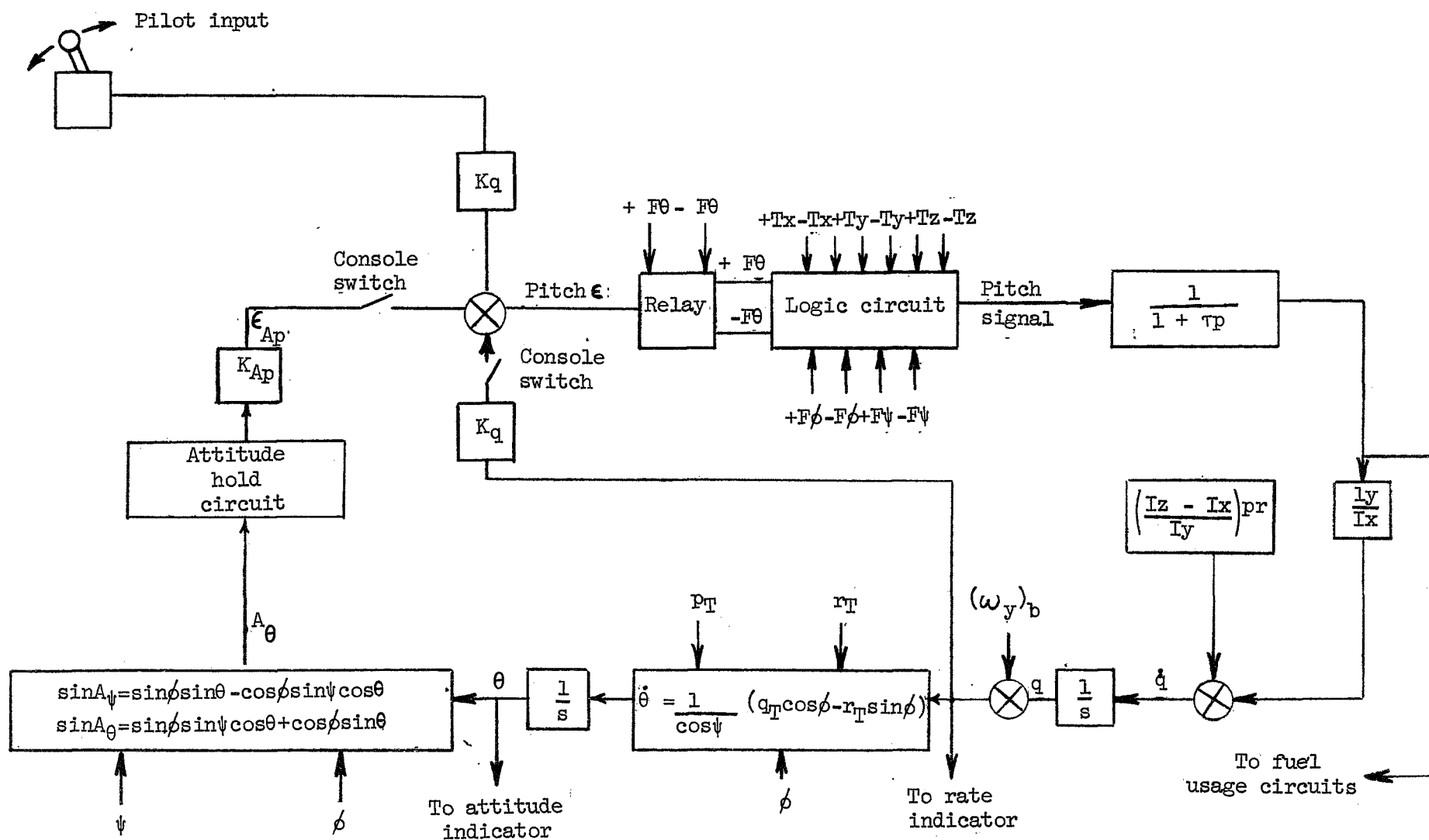


Figure 8 - Pitch Attitude Control Circuit (Att. Hold, Rate Command, and Open Loop).

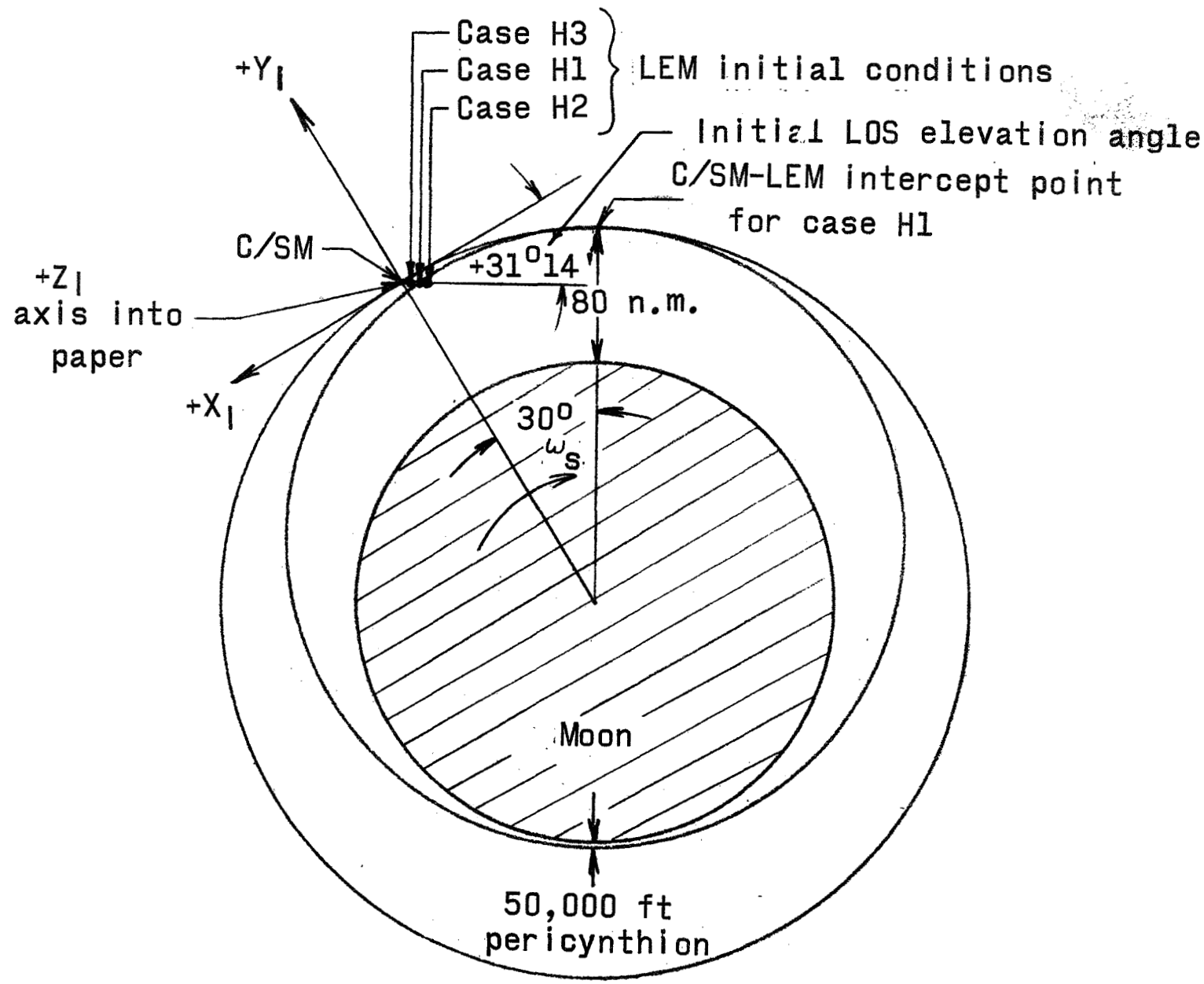


Figure 9.- Initial conditions for rendezvous from Hohmann type transfer cases.

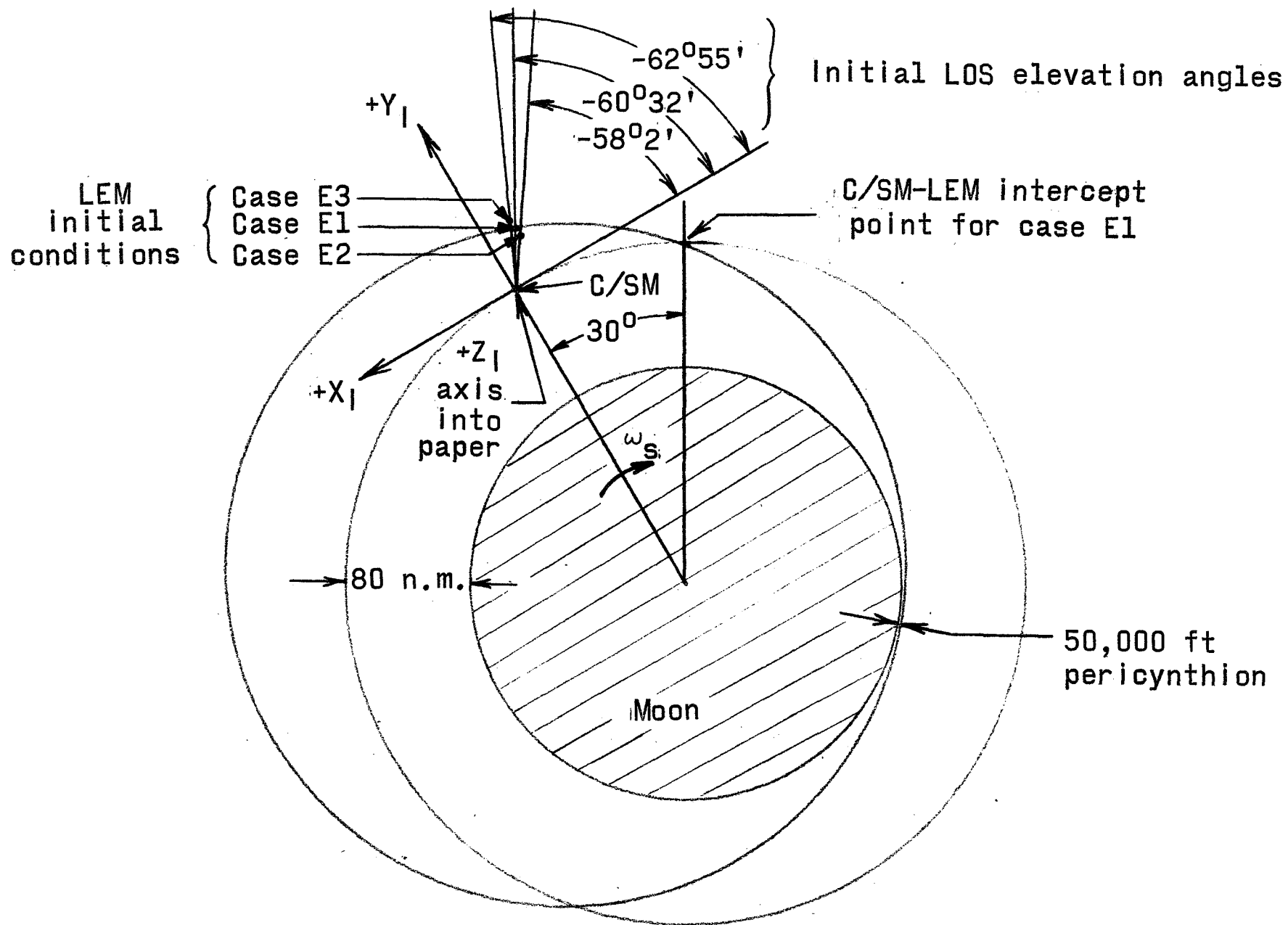


Figure 10.- Initial condition for rendezvous from equiperoid type transfer cases.

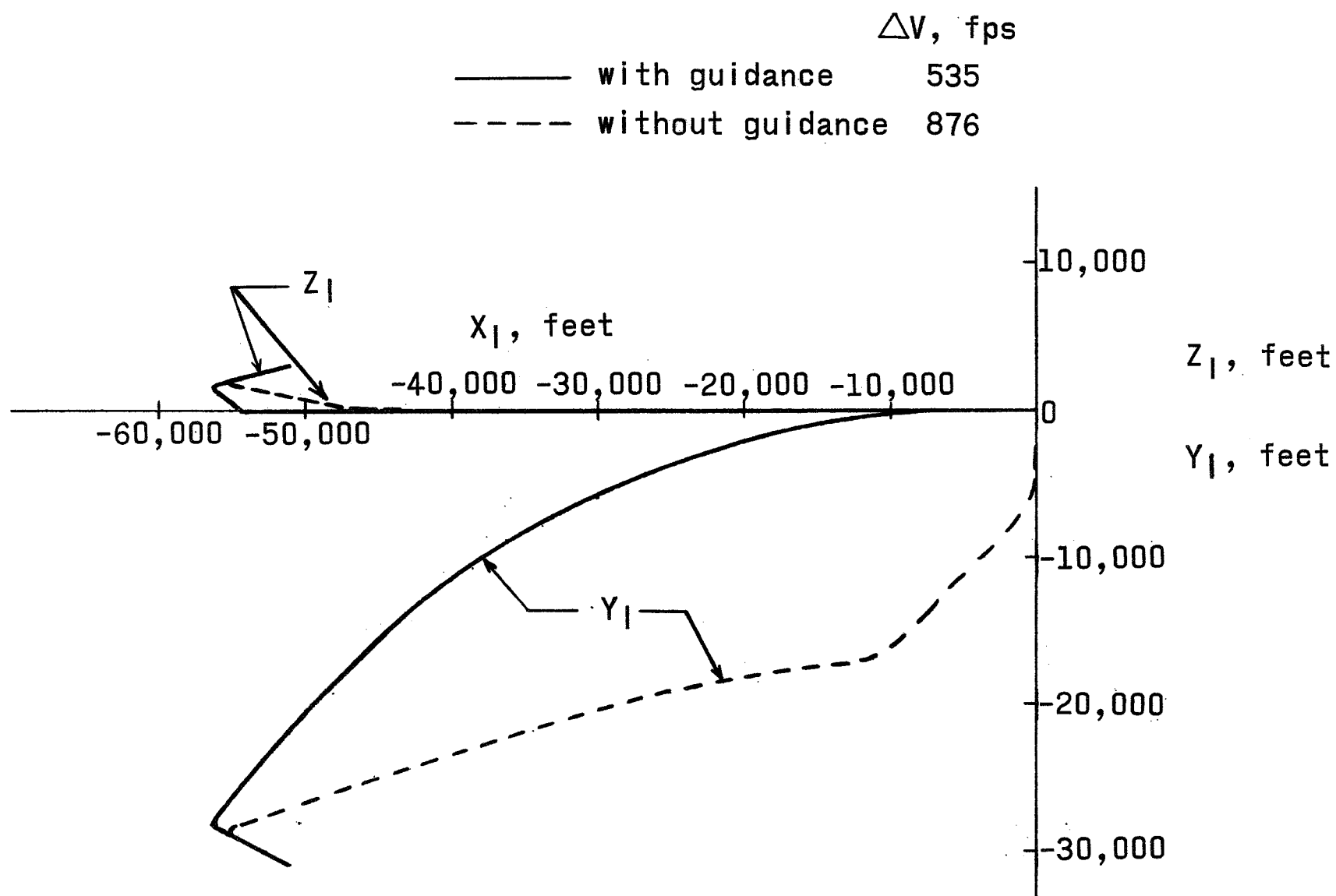


Figure 11.- Runs involving initial deviations from the Hohmann ellipse with and without guidance (case H3).

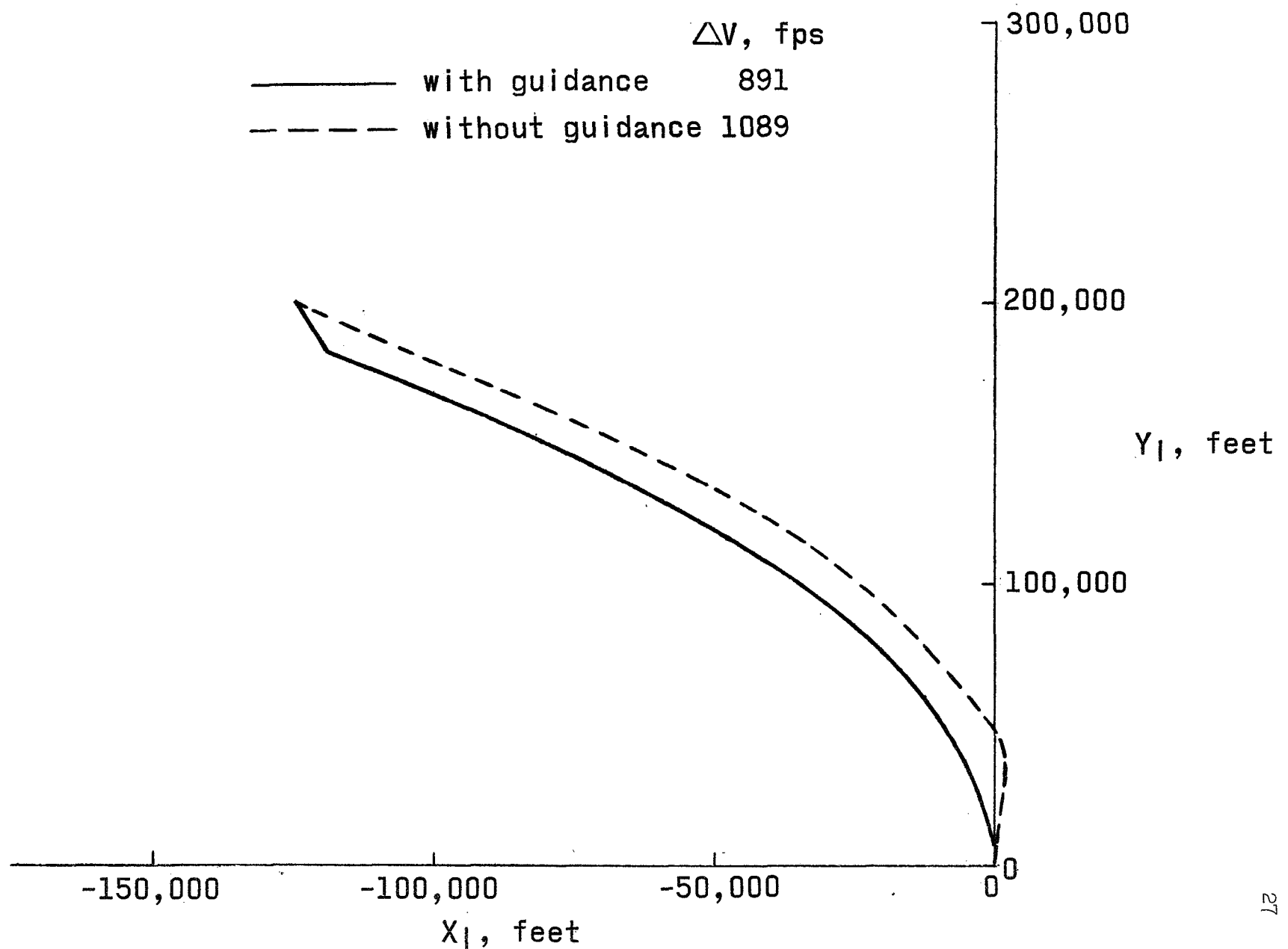
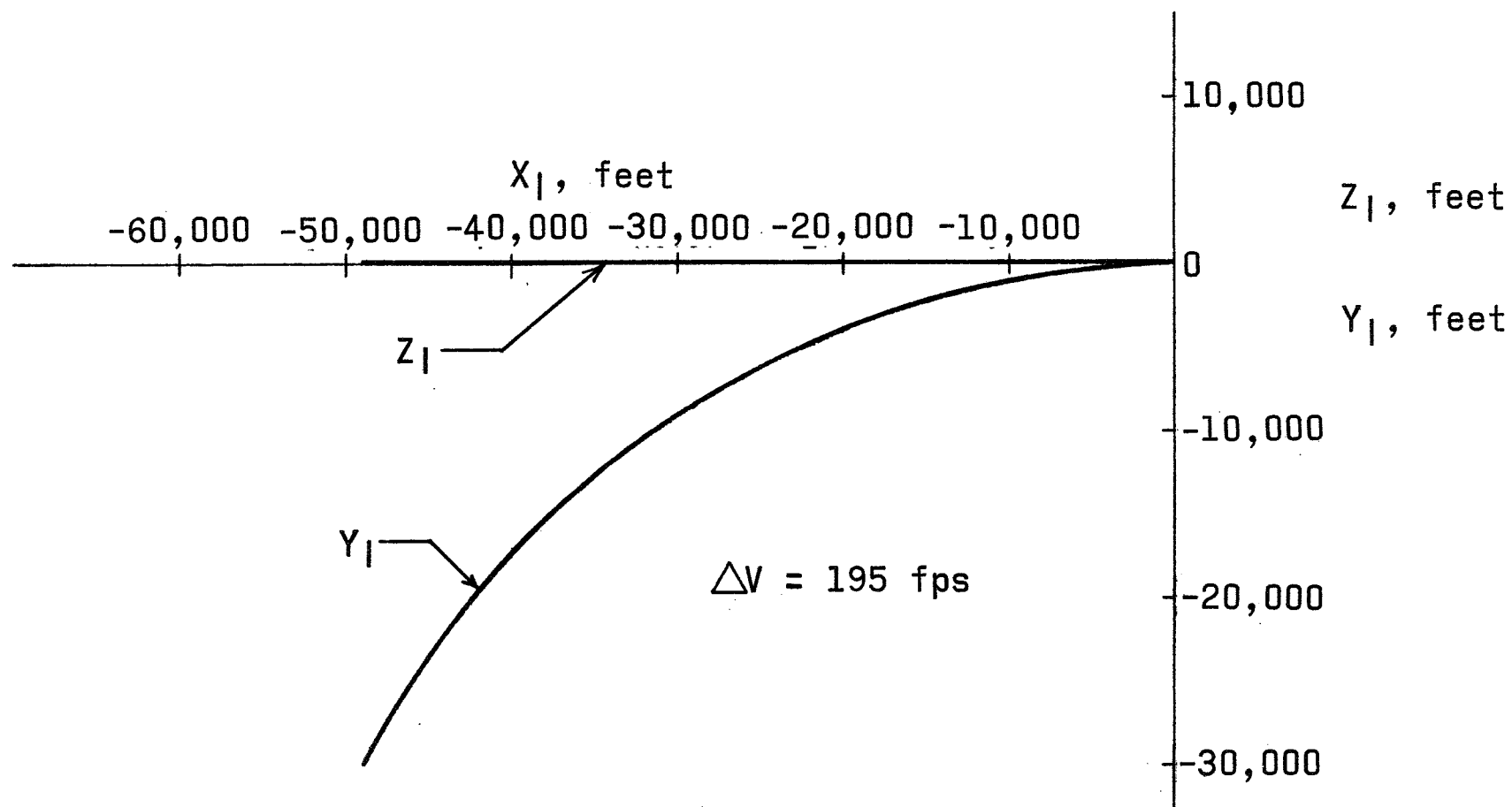


Figure 12.- Runs involving initial deviations from the equiperiod transfer ellipse with and without guidance (case E2).





(a) Typical trajectory flown with guidance (using ascent engine).

Figure 13.- Hohmann transfer rendezvous (case H1).

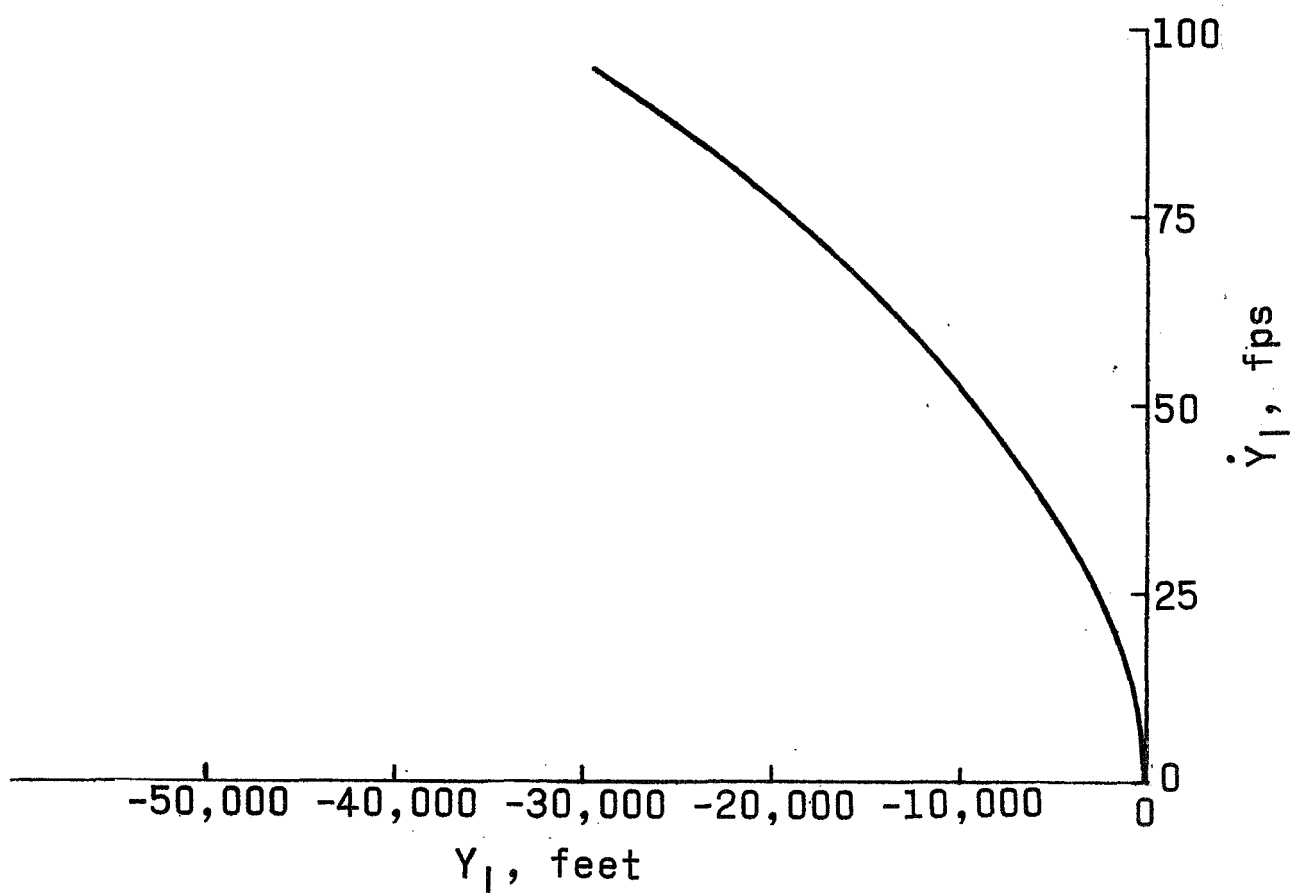
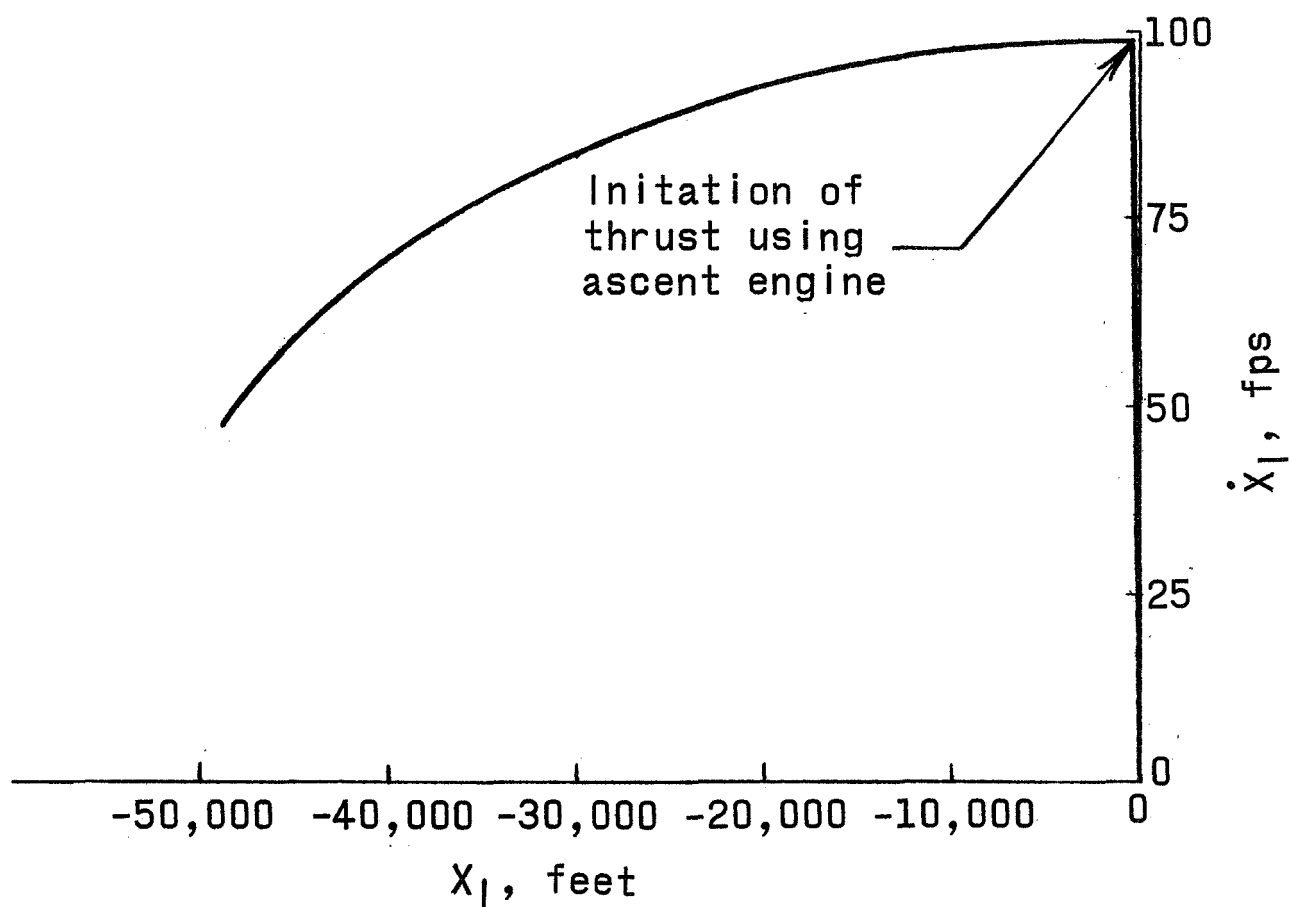
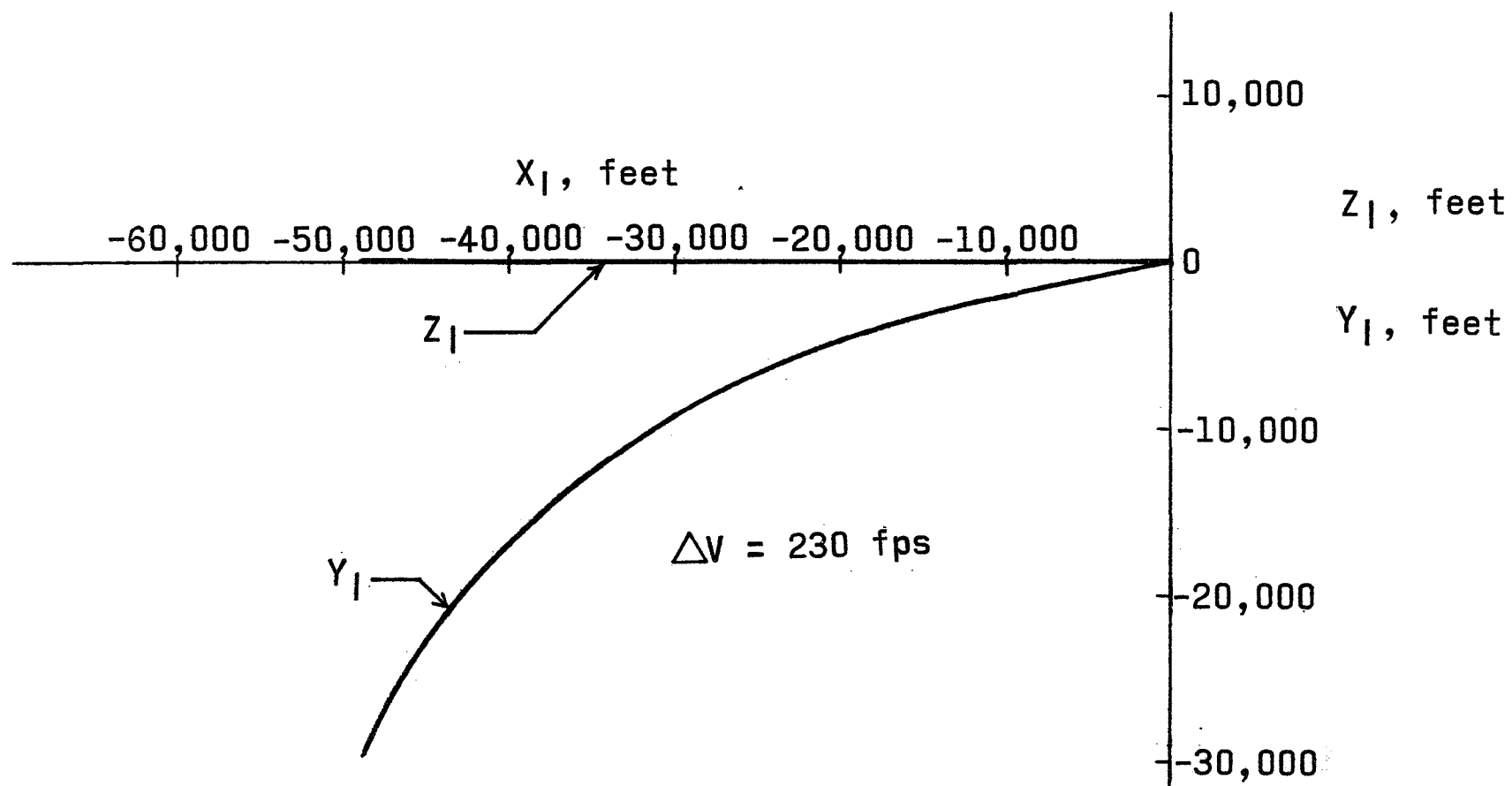


Figure 13.- Concluded. (b) Velocity profiles.



(a) Typical trajectory flown with guidance (using RCS jets).

Figure 14.- Hohmann transfer rendezvous (case H1).

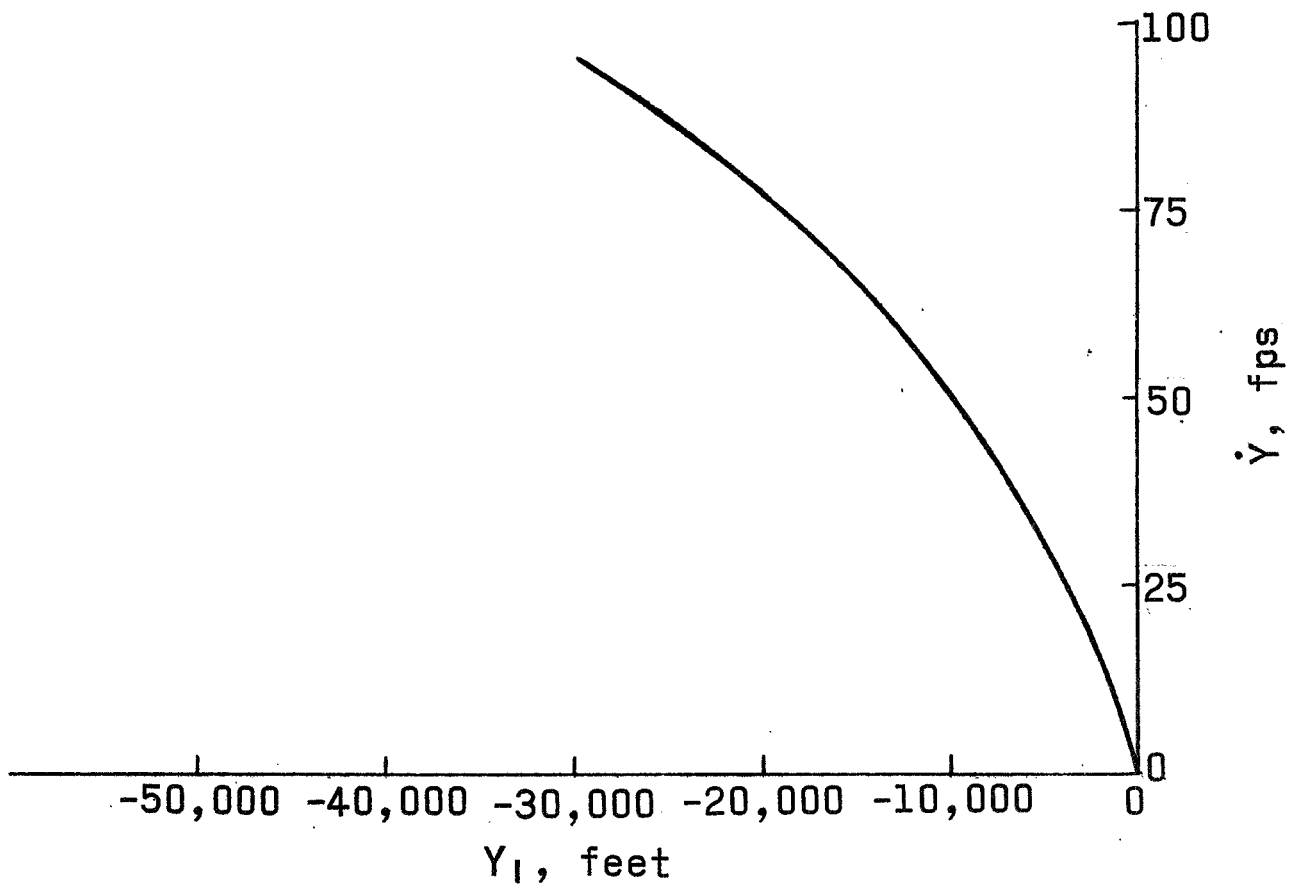
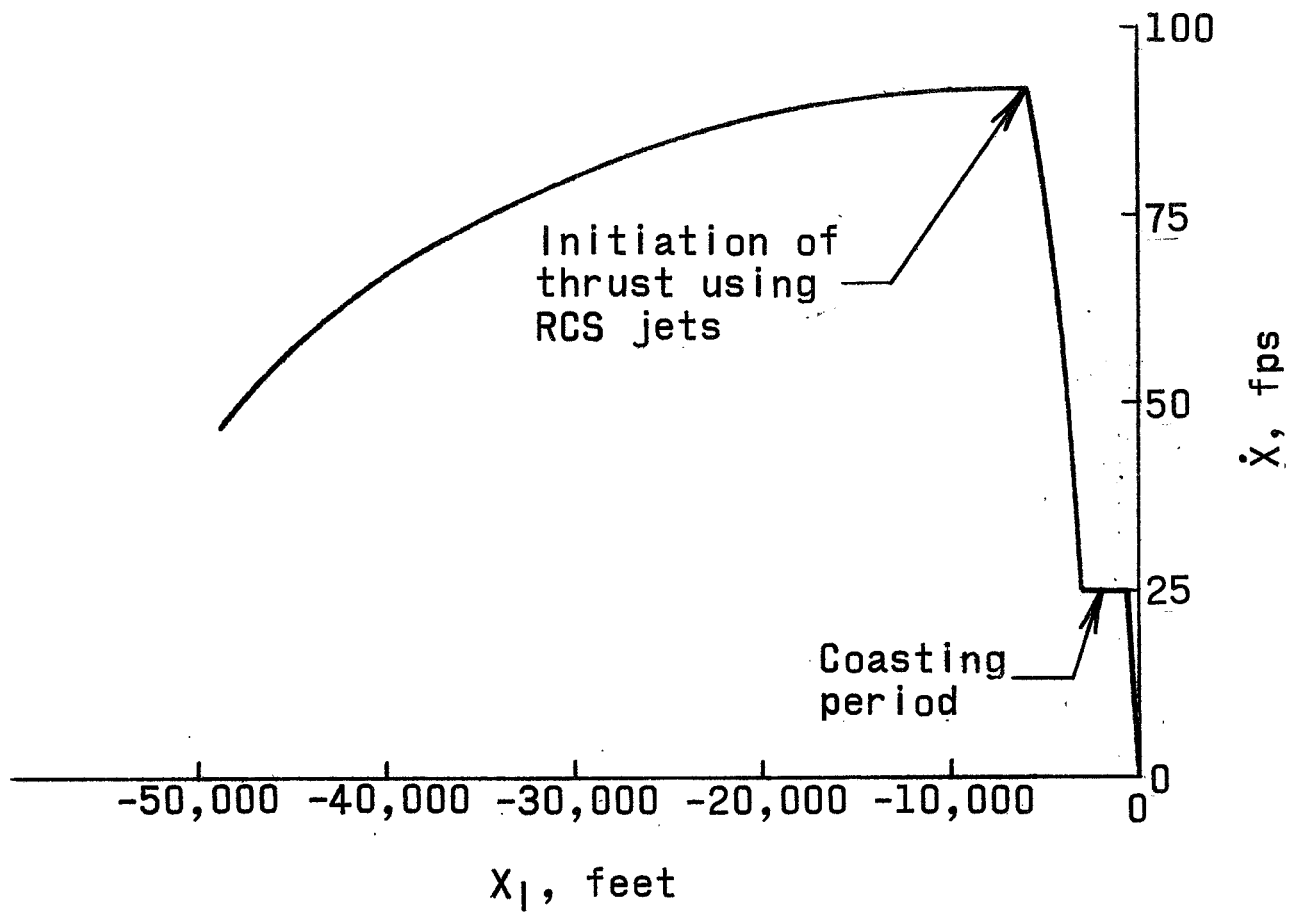
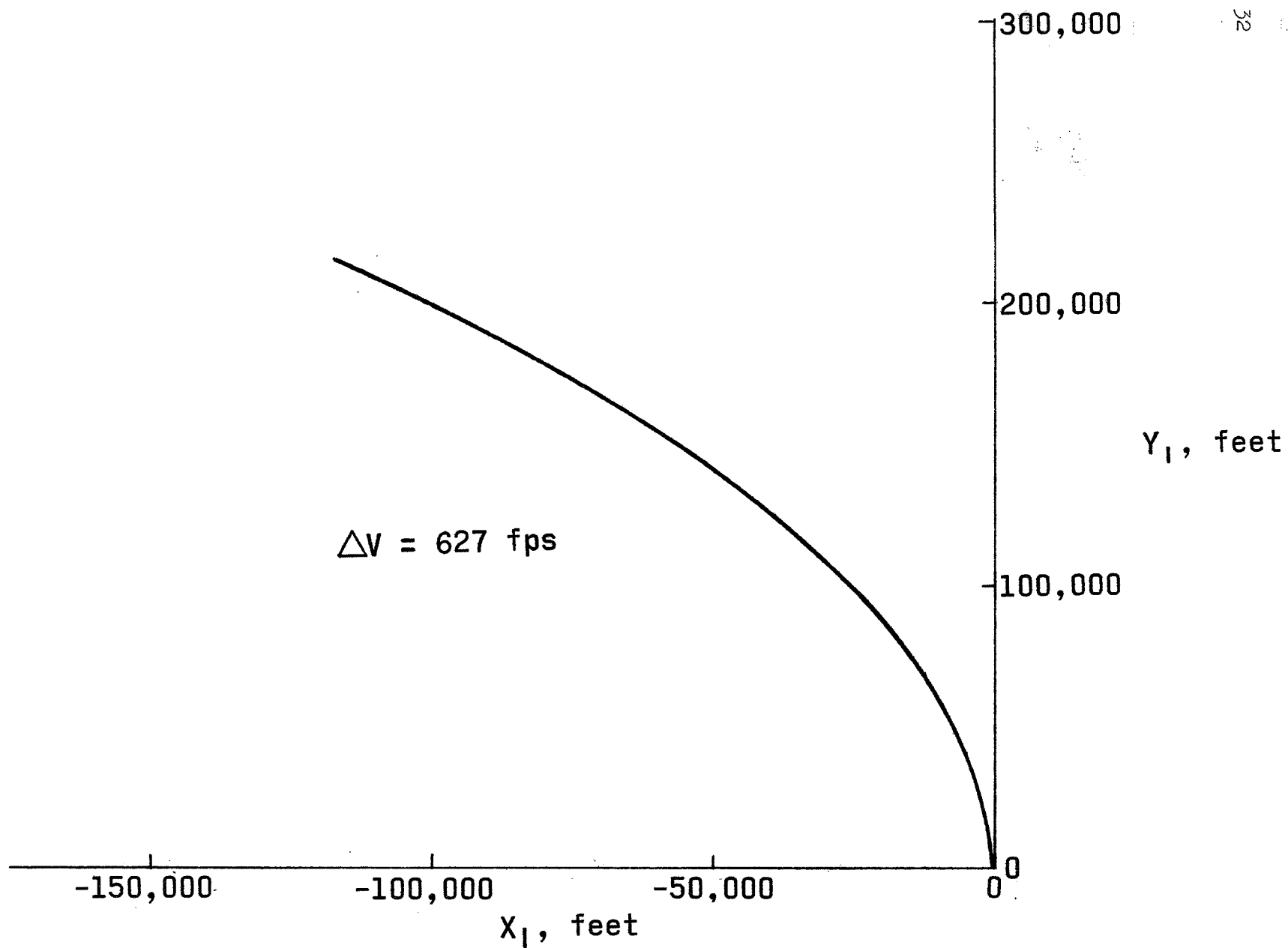


Figure 14.- Concluded.(b) Velocity profiles.



(a) Typical trajectory flown with guidance.  
Figure 15.- Equiperiod transfer rendezvous.

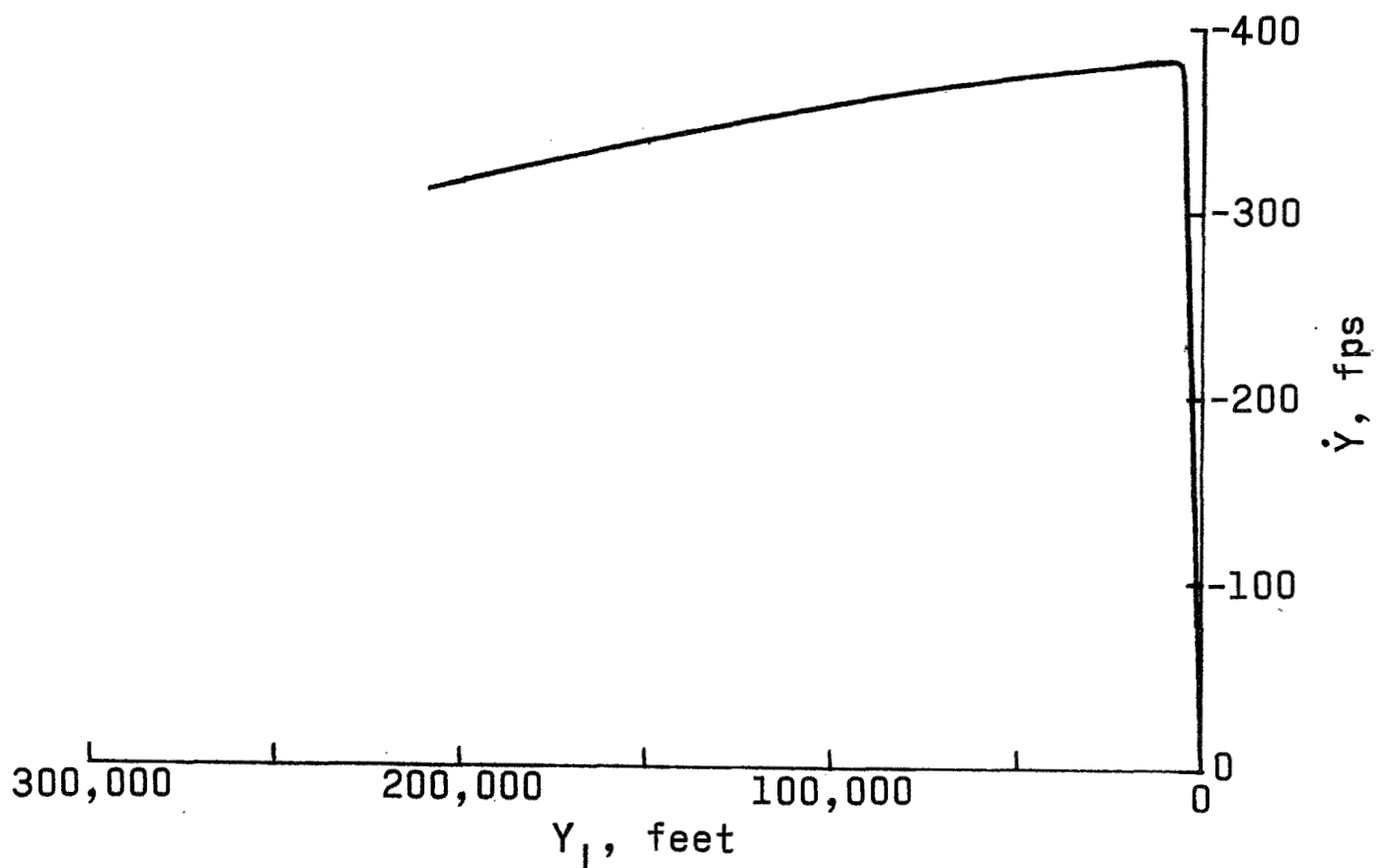
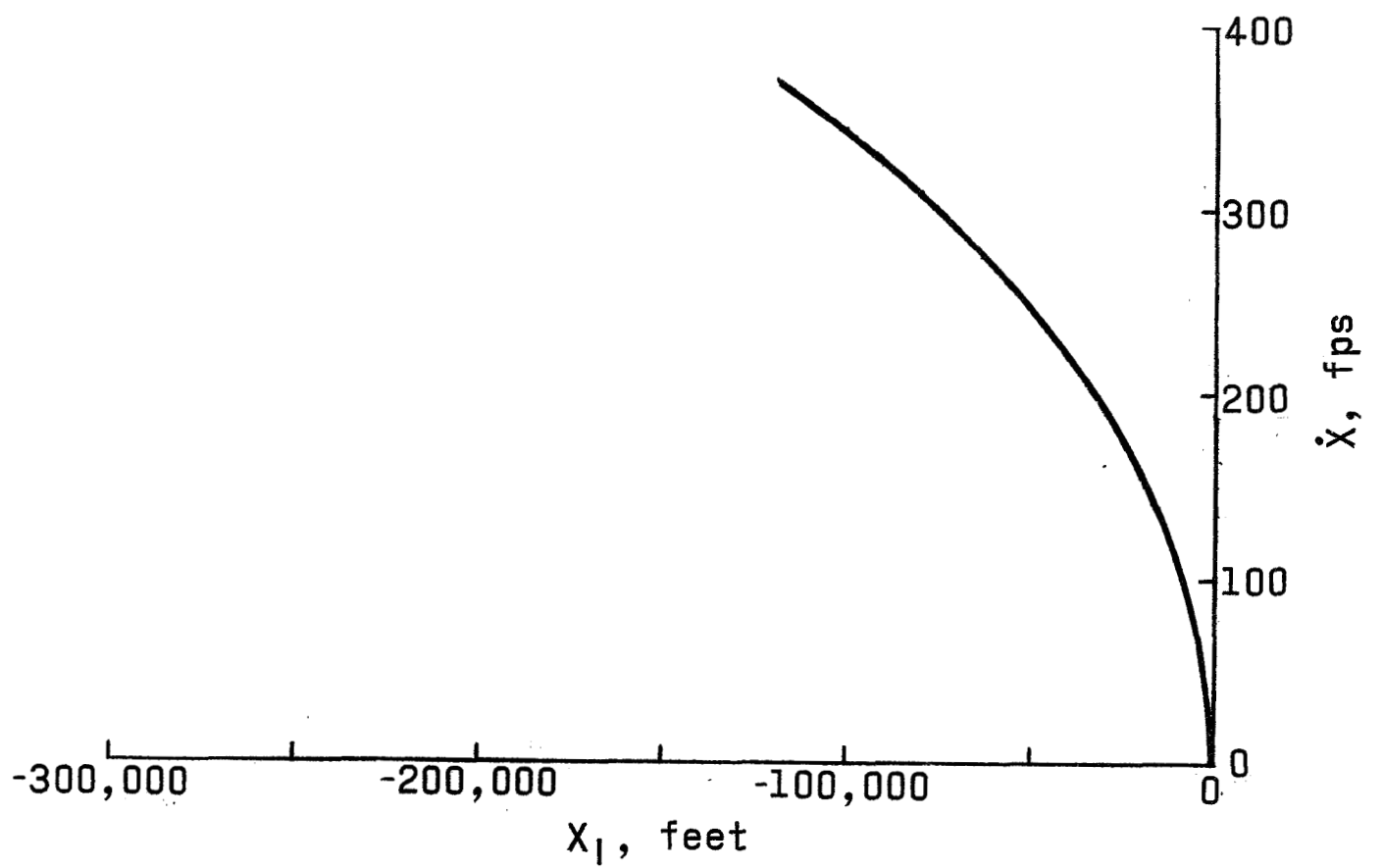


Figure 15.- Continued. (b) Velocity profiles.

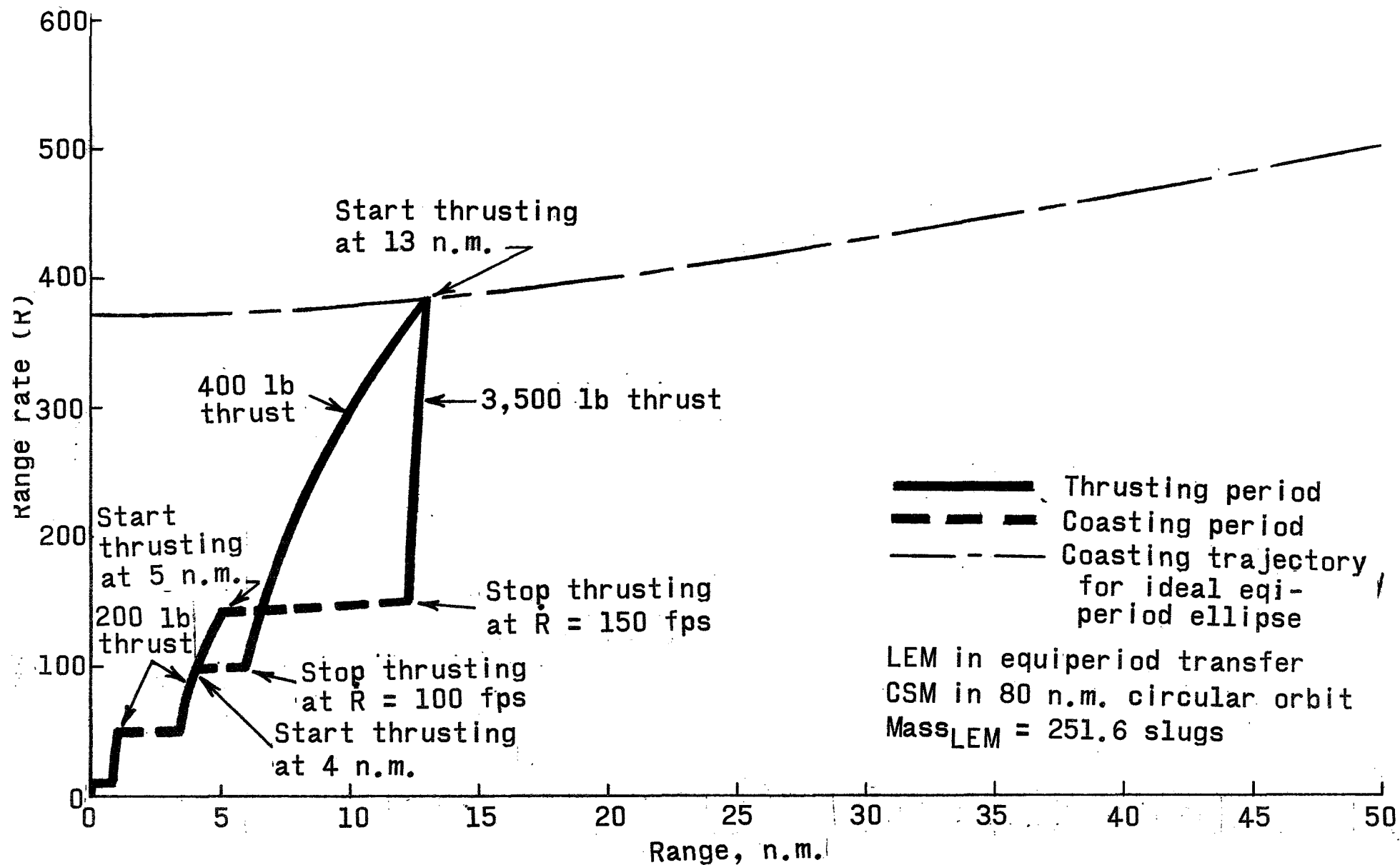


Figure 16.- Recommended thrusting schedule for equiperiod rendezvous.

## APPENDIX

## DEVELOPMENT OF GUIDANCE EQUATIONS

The linearized equations of motion of a mass measured in a rotating reference frame which moves in a circular orbit are given in ref. 3 as:

$$\ddot{X} - 2\omega\dot{Y} = \frac{T_{XI}}{m} \quad (A1)$$

$$\ddot{Y} + 2\omega\dot{X} - 3\omega^2 Y = \frac{T_{YI}}{m} \quad (A2)$$

$$\ddot{Z} + \omega^2 Z = \frac{T_{ZI}}{m} \quad (A3)$$

For zero thrust inputs, the solutions to equations (A1), (A2), and (A3) yield the following expressions for positions and velocities of the LEM relative to the CSM:

$$\begin{aligned} X_I = & 2 \left( \frac{2\dot{X}_O}{\omega_s} - 3Y_O \right) \sin \omega_s t - \frac{2\dot{Y}_O}{\omega_s} \cos \omega_s t \\ & + \left( 6Y_O - \frac{3\dot{X}_O}{\omega_s} \right) \omega_s t + \left( X_O + \frac{2\dot{Y}_O}{\omega_s} \right) \end{aligned} \quad (A4)$$

$$\begin{aligned} Y_I = & \left( \frac{2\dot{X}_O}{\omega_s} - 3Y_O \right) \cos \omega_s t + \frac{\dot{Y}_O}{\omega_s} \sin \omega_s t \\ & + \left( 4Y_O - \frac{2\dot{X}_O}{\omega_s} \right) \end{aligned} \quad (A5)$$

$$Z_I = Z_O \cos \omega_s t + \frac{\dot{Z}_O}{\omega_s} \sin \omega_s t \quad (A6)$$



$$\begin{aligned} \dot{X}_I = 2 \omega_s \left( \frac{2 \dot{X}_O}{\omega_s} - 3 Y_O \right) \cos \omega_s t \\ + 2 \dot{Y}_O \sin \omega_s t + \left( 6 \omega_s Y_O - 3 \dot{X}_O \right) \end{aligned} \quad (A7)$$

$$\dot{Y}_I = \left( 3 Y_O \omega_s - 2 \dot{X}_O \right) \sin \omega_s t + \dot{Y}_O \cos \omega_s t \quad (A8)$$

$$\dot{Z}_I = \frac{\dot{Z}_O}{\omega_s} \cos \omega_s t - Z_O \sin \omega_s t \quad (A9)$$

These equations therefore express the position and velocity of the ferry in terms of its initial conditions. If, however, the position of the LEM is known at any time, and intercept conditions are desired at some future time  $\tau$ , then it is required that the positions  $X_I$ ,  $Y_I$ ,  $Z_I$  be equal to zero when the elapsed time  $t$  is equal to  $\tau$ . Making these substitutions into equations (A4), (A5), and (A6) gives the following expressions for guidance velocities:

$$\dot{X}_O = \omega_s \left[ \frac{X_O \sin \omega_s \tau + Y_O [6 \omega_s \tau - 14(1 - \cos \omega_s \tau)]}{3 \omega_s \tau \sin \omega_s \tau - 8(1 - \cos \omega_s \tau)} \right] \quad (A10)$$

$$\dot{Y}_O = \omega_s \left[ \frac{2 X_O (1 - \cos \omega_s \tau) + Y_O (4 \sin \omega_s \tau - 3 \omega_s \tau \cos \omega_s \tau)}{3 \omega_s \tau \sin \omega_s \tau - 8(1 - \cos \omega_s \tau)} \right] \quad (A11)$$

$$\dot{Z}_O = - \frac{\omega_s Z_O}{\tan \omega_s \tau} \quad (A12)$$

By setting the values for the initial position ( $X_O$ ,  $Y_O$ ,  $Z_O$ ) equal to values of present position, determined by onboard radar and data processing equipment, equations (A10), (A11), and (A12) yield the velocities necessary for an intercept of the CSM by the LEM on a non-thrusting trajectory. These velocities were presented to the pilot as guidance velocities. Used in this manner the equations appear as:

$$\dot{X}_{RI} = \omega_s \left[ \frac{X_I \sin \omega_s \tau + Y_I [6 \omega_s \tau \sin \omega_s \tau - 14 (1 - \cos \omega_s \tau)]}{3 \omega_s \tau \sin \omega_s \tau - 8(1 - \cos \omega_s \tau)} \right] \quad (A13)$$

$$\dot{Y}_{RI} = \omega_s \left[ \frac{2 X_I (1 - \cos \omega_s \tau) + Y_I (4 \sin \omega_s \tau - 3 \omega_s \tau \cos \omega_s \tau)}{3 \omega_s \tau \sin \omega_s \tau - 8(1 - \cos \omega_s \tau)} \right] \quad (A14)$$

$$\dot{Z}_{RI} = - \frac{\omega_s Z_I}{\tan \omega_s \tau} \quad (A15)$$

$\omega_s$  = angular velocity of the rotating coordinate system relative to inertial space. (For the 80 nautical mile orbit about the moon,  $\omega_s = 8.5430495 \times 10^{-4}$  radians/sec)

To solve the equations of motion in the inertial frame of reference, the body thrusts were resolved into inertial components by the matrix transformation

$$\begin{Bmatrix} \frac{T_x}{m} \\ \frac{T_y}{m} \\ \frac{T_z}{m} \end{Bmatrix}_I = A(\theta, \psi, \phi) \begin{Bmatrix} \frac{T_x}{m} \\ \frac{T_y}{m} \\ \frac{T_z}{m} \end{Bmatrix}_b \quad (A16)$$

where "b" denotes the LEM body axis system (see fig. 6) and "I" denotes the CSM centered reference axis system.

The LEM body angular rates were obtained by integrating the following angular acceleration equations with respect to time:

$$p = \int \frac{M_\phi + (I_{yb} - I_{zb}) qr}{I_{xb}} dt \quad (A17)$$

$$q = \int \frac{M_\theta + (I_{zb} - I_{xb}) rp}{I_{yb}} dt \quad (A18)$$

$$r = \int \frac{M_\psi + (I_{xb} - I_{yb}) pq}{I_{zb}} dt \quad (A19)$$

These equations are solved simultaneously on the analog computer. Superimposed upon these angular rates were the components of the inertial coordinate system rotational rate referred to the LEM body axis system by the matrix transformation

$$\begin{Bmatrix} \omega_X \\ \omega_Y \\ \omega_Z \end{Bmatrix}_b = \begin{bmatrix} & & \\ & & \\ & & \end{bmatrix}^{-1} \begin{Bmatrix} 0 \\ \omega_s \\ 0 \end{Bmatrix} \quad (A20)$$

$A(\theta, \psi, \phi)$

therefore, the total angular rates of the LEM body axis system relative to the inertial axis system were defined as

$$p_T = p + \omega_X \quad (A21)$$

$$q_T = q + \omega_Y \quad (A22)$$

$$r_T = r + \omega_Z \quad (A23)$$

Using these LEM body angular rates, the Euler angle rates were determined by solving the equations shown on the following page:

$$\dot{\theta} = \frac{q_T \cos \phi - r_T \sin \phi}{\cos \psi} \quad (\text{A24})$$

$$\dot{\psi} = q_T \sin \phi + r_T \cos \phi \quad (\text{A25})$$

$$\dot{\phi} = p_T - \dot{\theta} \sin \psi \quad (\text{A26})$$

In this manner the Euler angles were constantly updated for use in the matrix transformations. These Euler angles were also displayed on the visual all-attitude indicator.